The gut microbiome regulates memory function

Emily E Noble[1], Christine A. Olson[3], Elizabeth Davis[2], Linda Tsan[2], Yen-Wei Chen[3], Ruth Schade[1], Clarissa Liu[2], Andrea Suarez[2], Roshonda B Jones[2], Michael I Goran[2], Claire de La Serre[1], Xia Yang[3], *Elaine Y. Hsiao[3] and *Scott E Kanoski[2]

[1]University of Georgia, Athens, Georgia, USA; [2]University of Southern California, Los Angeles, California, USA; [3]University of California, Los Angeles, California, USA

*Correspondence (Lead Contact):
Scott E. Kanoski, Ph.D
University of Southern California
Email: kanoski@usc.edu
Or
*Elaine Y. Hsiao, Ph.D (Co-Corresponding Author)
University of California Los Angeles
Email: ehsiao@ucla.edu

Abstract:

Emerging evidence highlights a critical relationship between gut microbiota and neurocognitive development. Here we explore whether excessive early life consumption of added sugars negatively impacts neurocognitive development via the gut microbiome. Using a rodent model of sugar-sweetened beverage (SSB) consumption during adolescence, we show that excessive early life sugar intake impairs adult hippocampal-dependent memory function while preserving other neurocognitive domains. Adolescent SSB consumption during adolescence also elevates fecal microbial abundance of *Parabacteroides*, which negatively correlates with memory task performance. Transferred enrichment of *Parabacteroides* species *P. distasonis* and *P. johnsonii* in adolescent rats impairs memory function during adulthood. Hippocampus transcriptome analyses identify gene expression alterations in neurotransmitter synaptic signaling, intracellular kinase signaling, metabolic function, neurodegenerative disease, and dopaminergic synaptic signaling-associated pathways as potential mechanisms linking bacterial alterations with memory impairment. Collectively these results identify a role for microbiota "dysbiosis" in mediating the negative effects of early life unhealthy dietary factors on neurocognitive outcomes.

43 **Introduction:**
44

45 The gut microbiome has recently been implicated in modulating neurocognitive
46 development and consequent functioning [1, 2]. Early life developmental periods represent
47 critical windows for the impact of indigenous gut microbes on the brain, as evidenced by
48 the reversal of behavioral and neurochemical abnormalities in germ free rodents when
49 inoculated with conventional microbiota during early life, but not during adulthood [3-5].
50 Dietary factors are a critical determinant of gut microbiota diversity and can alter gut
51 bacterial communities, as evident from the microbial plasticity observed in response to
52 pre- and probiotic treatment, as well as the "dysbiosis" resulting from consuming
53 unhealthy, yet palatable foods that are associated with obesity and metabolic disorders
54 (e.g., "Western diet"; foods high in saturated fatty acids and added sugar) [6]. In addition
55 to altering the gut microbiota, consumption of these dietary factors yields long-lasting
56 memory impairments, and these effects are more pronounced when consumed during
57 early life developmental periods vs. during adulthood [7-9]. Whether diet-induced changes
58 in specific bacterial populations are functionally related to altered early life
59 neurocognitive outcomes, however, is poorly understood.
60

61 The hippocampus, which is well known for its role in spatial and episodic memory and
62 more recently for regulating learned and social aspects of food intake control [10-15], is
63 particularly vulnerable to the deleterious effects of Western dietary factors [16-18]. During
64 the juvenile and adolescent stages of development, a time when the brain is rapidly
65 developing, consumption of diets high in saturated fat and sugar [19-21] or sugar alone [22-25]
66 impairs hippocampal function while in some cases preserving memory processes that do

not rely on the hippocampus. While several putative underlying mechanisms have been investigated, the precise biological pathways linking dietary factors to neurocognitive dysfunction remain largely undetermined [9]. Here we aimed to determine whether sugar-induced alterations in gut microbiota during early life are causally related to hippocampal-dependent memory impairments observed during adulthood.

Methods and Materials:

Experimental Subjects

Juvenile male Sprague Dawley rats (Envigo; arrival post natal day (PN) 26-28; 50-70g) were housed individually in standard conditions with a 12:12 light/dark cycle. All rats had ad libitum access to water and Lab Diet 5001 (PMI Nutrition International, Brentwood, MO; 29.8 % kcal from protein, 13.4% kcal from fat, 56.7% kcal from carbohydrate), with modifications where noted. All experiments were performed in accordance with the approval of the Animal Care and Use Committee at the University of Southern California.

Experiment 1

Twenty one juvenile male rats (PN 26-28) were divided into two groups with equal body weight and given ad libitum access to: 1) 11% weight-by-volume (w/v) solution containing monosaccharide ratio of 65% fructose and 35% glucose in reverse osmosis-filtered water (SUG; n=11) or 2) or an extra bottle of reverse osmosis-filtered water (CTL; n=10). This solution was chosen to model commonly consumed sugar-sweetened beverages in humans in terms of both caloric content and monosaccharide ratio[26].

91 Additionally, all rats were given ad libitum access to water and standard rat chow. Food
92 intake, solution intake and body weights were monitored thrice weekly except where
93 prohibited due to behavioral testing. At PN 60, rats underwent Novel Object in Context
94 (NOIC) testing, to measure hippocampal-dependent episodic contextual memory. At PN
95 67 rats underwent anxiety-like behavior testing in the Zero Maze, followed by body
96 composition testing at PN 70 and an intraperitoneal glucose tolerance test (IP GTT) at
97 PN 84. All behavioral procedures were run at the same time each day (4-6 hours into the
98 light cycle). Fecal and cecal samples were collected prior to sacrifice at PN 104.
99
100 In a separate cohort of juvenile male rats (n=6/group) animals were treated as above,
101 but on PN day 60 rats were tested in the Novel Object Recognition (NOR) and Open
102 Field (OF) tasks, with two days in between tasks. Animals were sacrificed and tissue
103 punches were collected from the dorsal hippocampus on PN day 65. Tissue punches
104 were flash frozen in isopentane packed in dry ice and stored at -80°C until further
105 analyses.
106
107 **Experiment 2**
108 Twenty-three juvenile male rats (PN 26-28) were divided into two groups and received a
109 gavage twice daily (12 hours apart) for 7 days (only one treatment was given on day 7) of
110 either (1) saline (SAL; n=8), or (2) a cocktail of antibiotics consisting of Vancomycin (50
111 mg/kg), Neomycin (100 mg/kg), and Metronidazole (100 mg/kg) along with
112 supplementation with 1 mg/mL of ampicillin in their drinking water (ABX; n=15), which
113 is a protocol modified from [27]. Animals were housed in fresh, sterile cages on Day 3 of
114 the antibiotic or saline treatment, and again switched to fresh sterile cages on Day 7

115 after the final gavage. All animals were maintained on sterile, autoclaved water and
116 chow for the remainder of the experiment. Rats in the ABX group were given water
117 instead of ampicillin solution on Day 7. Animals in the ABX group were further
118 subdivided to receive either gavage of a 1:1 ratio of *Parabacteroides distasonis* and
119 *Parabacteroides johnsonii* (PARA; n=8) or saline (SAL; n=7) thirty six hours after the
120 last ABX treatment. To minimize potential contamination, rats were handled minimally
121 for 14 days. Cage changes occurred once weekly at which time animals and food were
122 weighed. Experimenters wore fresh, sterile PPE and weigh boxes were cleaned with
123 sterilizing solution in between each cage change. On PN 50 rats were tested in NOIC, on
124 PN 60 rats were tested in NOR, on PN 62 rats were tested in the Zero Maze, followed by
125 Open Field on PN 64. On PN 73 rats were given an IP GTT, and on PN 76 body
126 composition was tested. Rats were sacrificed at PN 83 and dorsal hippocampus tissue
127 punches were collected on PN day 65. Tissue punches were flash frozen in isopentane
128 packed in dry ice and stored at -80°C until further analyses.
129

130 **IP glucose tolerance test (IP GTT)**

131 Animals were food restricted 24 hours prior to IP GTT. Immediately prior to the test,
132 baseline blood glucose readings were obtained from tail tip and recorded by a blood
133 glucose meter (One touch Ultra2, LifeScan Inc., Milpitas, CA). Each animal was then
134 intraperitoneally (IP) injected with dextrose solution (0.923g/ml by body weight) and
135 tail tip blood glucose readings were obtained at 30, 60, 90, and 120 min after IP
136 injections, as previously described [22].
137

138 **Zero Maze**

The Zero Maze is an elevated circular track (63.5 cm fall height, 116.8cm outside diameter), divided into four equal length sections. Two sections were open with 3 cm high curbs, whereas the 2 other closed sections contained 17.5 cm high walls. Animals are placed in the maze facing the open section of the track in a room with ambient lighting for 5 min while the experimenter watches the animal from a monitor outside of the room. The experimenter records the total time spent in the open sections (defined as the head and front two paws in open arms), and the number of crosses into the open sections from the closed sections.

Novel object in context task (NOIC)

NOIC measures episodic contextual memory based on the capacity for an animal to identify which of two familiar objects it has never seen before in a specific context. Procedures were adapted from prior reports [28, 29]. Briefly, rats are habituated to two distinct contexts on subsequent days (with the habituation order counterbalanced by group) for 5-min sessions: Context 1 is a semi-transparent box (15in W x 24in L x 12in H) with orange stripes and Context 2 is a grey opaque box (17in W x 17in L x 16in H) (Context identify assignments counterbalanced by group), each context is in a separate dimly lit room, which is obtained using two desk lamps pointed toward the floor . Day 1 of NOIC begins with each animal being placed in Context 1 containing two distinct similarly sized objects placed in opposite corners: a 500ml jar filled with blue water (Object A) and a square glass container (Object B) (Object assignments and placement counterbalanced by group). On day 2 of NOIC, animals are placed in Context 2 with duplicates of one of the objects. On NOIC day 3, rats are placed in Context 2 with Objects A and Object B. One of these objects is not novel to the rat, but its placement in

Context 2 is novel. All sessions are 5 minutes long and are video recorded. Each time the rat is placed in one of the contexts, it is placed with its head facing away from both objects. The time spent investigating each object is recorded from the video recordings by an experimenter who is blinded to the treatment groups. Exploration is defined as sniffing or touching the object with the nose or forepaws. The task is scored by calculating the time spent exploring the Novel Object to the context divided by the time spent exploring both Objects A and B combined, which is the novelty or "discrimination index". Rats with an intact hippocampus will preferentially investigate the object that is novel to Context 2, given that this object is a familiar object yet is now presented in a novel context, whereas hippocampal inactivation impairs the preferential investigation of the object novel to Context 2 [28].

Novel Object Recognition

The apparatus used for NOR is a grey opaque box (17in W x 17in L x 16in H) placed in a dimly lit room, which is obtained using two desk lamps pointed toward the floor. Procedures are adapted from [30]. Rats are habituated to the empty arena and conditions for 10 minutes on the day prior to testing. The novel object and the side on which the novel object is placed is counterbalanced by group. The test begins with a 5-minute familiarization phase, where rats are placed in the center of the arena, facing away from the objects, with two identical copies of the same object to explore. The objects were either two identical cans or two identical bottles, counterbalanced by treatment group. The objects were chosen based on preliminary studies which determined that they are equally preferred by Sprague Dawley rats. Animals are then removed from the arena and placed in the home cage for 5 minutes. The arena and objects are cleaned with 10%

187 ethanol solution, and one of the objects in the arena is replaced with a different one
188 (either the can or bottle, whichever the animal has not previously seen, i.e., the "novel
189 object"). Animals are again placed in the center of the arena and allowed to explore for 3
190 minutes. Time spent exploring the objects is recorded via video recording and analyzed
191 using Any-maze activity tracking software (Stoelting Co., Wood Dale, IL).
192
193 **Open Field**
194 Open field measures general activity level and also anxiety-like behavior in the rat. A
195 large gray bin, 60 cm (L) X 56 CM (W) is placed under diffuse even lighting (30 lux). A
196 center zone is identified and marked in the bin (19 cm L X 17.5 cm W). A video camera is
197 placed directly overhead and animals are tracked using AnyMaze Software (Stoelting
198 Co., Wood Dale, IL). Animals are placed in the center of the box facing the back wall and
199 allowed to explore the arena for 10 min while the experimenter watches from a monitor
200 in an adjacent room. The apparatus is cleaned with 10% ethanol after each rat is tested.
201
202 **Body Composition**
203 Body composition (body fat, lean mass) was measured using LF90 time domain nuclear
204 magnetic resonance (Bruker NMR minispec LF 90II, Bruker Daltonics, Inc.).
205
206 **Bacterial transfer**
207 *Parabacteroides distasonis* (ATCC 8503) was cultured under anaerobic conditions at
208 37C in Reinforced Clostridial Medium (RCM, BD Biosciences). *Parabacteroides*
209 *johnsonii* (DSM 18315) was grown in anaerobic conditions in PYG medium (modified,
210 DSM medium 104). Cultures were authenticated by full-length 16S rRNA gene

211 sequencing. For bacterial enrichment, 10^9 colony-forming units of both *P. distasonis*
212 and *P. johnsonii* were suspended in 500 uL pre-reduced PBS and orally gavaged into
213 antibiotic-treated rats. When co-administered, a ratio of 1:1 was used for *P. distasonis*
214 and *P. johnsonii*.
215

216 **Gut microbiota DNA extraction and 16s rRNA gene sequencing in sugar-fed**
217 **and control rats**

218 All samples were extracted and sequenced according to the guidelines and procedures
219 established by the Earth Microbiome Project [31]. DNA was extracted from fecal and cecal
220 samples using the MO BIO PowerSoil DNA extraction kit. PCR targeting the V4 region
221 of the 16S rRNA bacterial gene was performed with the 515F/806R primers, utilizing the
222 protocol described in Caporaso et al.[32]. Amplicons were barcoded and pooled in equal
223 concentrations for sequencing. The amplicon pool was purified with the MO BIO
224 UltraClean PCR Clean-up kit and sequenced by the 2 x 150bp MiSeq platform at the
225 Institute for Genomic Medicine at UCSD. All sequences were deposited in Qiita Study
226 11255 as raw FASTQ files. Sequences were demultiplexed using Qiime-1 based "split
227 libraries" with the forward reads only dropping. Demultiplexed sequences were then
228 trimmed evenly to 100 bp and 150 bp to enable comparison to other studies for meta
229 analyses. Trimmed sequences were matched to known OTUs at 97% identity.
230

231 **Gut microbiota DNA extraction and 16S rRNA gene sequencing for**
232 ***Parabacteroides*-enriched and control rats**

233 Total bacterial genomic DNA was extracted from rat fecal samples (0.25 g) using the
234 Qiagen DNeasy PowerSoil Kit. The library was prepared following methods from

235 (Caporaso et al., 2011). The V4 region (515F-806R) of the 16S rDNA gene was PCR
236 amplified using individually barcoded universal primers and 30 ng of the extracted
237 genomic DNA. The conditions for PCR were as follows: 94°C for 3 min to denature the
238 DNA, with 35 cycles at 94°C for 45 s, 50°C for 60 s, and 72°C for 90 s, with a final
239 extension of 10 min at 72°C. The PCR reaction was set up in triplicate, and the PCR
240 products were purified using the Qiaquick PCR purification kit (QIAGEN). The purified
241 PCR product was pooled in equal molar concentrations quantified by nanodrop and
242 sequenced by Laragen, Inc. using the Illumina MiSeq platform and 2 x 250bp reagent
243 kit for paired-end sequencing. Amplicon sequence variants (ASVs) were chosen after
244 denoising with the Deblur pipeline. Taxonomy assignment and rarefaction were
245 performed using QIIME2-2019.10.
246
247 **Hippocampal RNA extraction and sequencing**
248 Hippocampi from rats treated with or without sugar or *Parabacteroides* were subject to
249 RNA-seq analysis. Total RNA was extracted according to manufacturer's instructions
250 using RNeasy Lipid Tissue Mini Kit (Qiagen, Hilden, Germany). Total RNA was checked
251 for degradation in a Bioanalyzer 2100 (Agilent, Santa Clara, CA, USA). Quality was very
252 high for all samples, and libraries were prepared from 1 ug of total RNA using a NuGen
253 Universal Plus mRNA-seq Library Prep Kit (Tecan Genomics Inc. Redwood City, CA).
254 Final library products were quantified using the Qubit 2.0 Fluorometer (Thermo Fisher
255 Scientific Inc., Waltham, MA, USA), and the fragment size distribution was determined
256 with the Bioanalyzer 2100. The libraries were then pooled equimolarly, and the final
257 pool was quantified via qPCR using the Kapa Biosystems Library Quantification Kit,
258 according to manufacturer's instructions. The pool was sequenced in an Illumina

259 NextSeq 550 platform (Illumina, San Diego, CA, USA), in Single-Read 75 cycles format,
260 obtaining about 25 million reads per sample. The preparation of the libraries and the
261 sequencing was performed at the USC Genome Core (http://uscgenomecore.usc.edu/)
262

263 **RNA-seq quality control**

264 Data quality checks were performed using the FastQC tool
265 (http://www.bioinformatics.babraham.ac.uk/projects/fastqc) and low quality reads
266 were trimmed with Trim_Galore
267 (http://www.bioinformatics.babraham.ac.uk/projects/trim_galore/). RNA-seq reads
268 passing quality control were mapped to *Rattus novegicus* transcriptome (Rnor6) and
269 quantified with Salmon [33]. Salmon directly mapped RNA-seq reads to Rat
270 transcriptome and quantified transcript counts. Txiimport [34] were used to convert
271 transcript counts into gene counts. Potential sample outliers were detected by principle
272 component analysis (PCA) and one control and one treatment sample from the
273 *Parabacteroides* experiment were deemed outliers (Figure S7A, B) and removed.
274

275 **Identification of differentially expressed genes (DEGs)**

276 DESeq2[35] were used to conduct differential gene expression analysis between sugar
277 treatment and the corresponding controls, or between *Parabacteroides* treatment and
278 the corresponding controls. Low-abundance genes were filtered out and only those
279 having a mean raw count > 1 in more than 50% of the samples were included.
280 Differentially expressed genes were detected by DESeq2 with default settings.
281 Significant DEGs were defined as Benjamini-Hochberg (BH) adjusted false discovery
282 rate (FDR) < 0.05. For heatmap visualization, genes were normalized with variance

283 stabilization transformation implemented in DESeq2, followed by calculating a z-score
284 for each gene.
285
286 **Pathway analyses of DEGs**
287 For the pathway analyses, DEGs at p-value < 0.01 was used. Pathway enrichment
288 analysis were conducted using enrichr[36] by intersecting each signature with pathways or
289 gene sets from KEGG[37], gene ontology biological pathways (GOBP), Cellular Component
290 (GOCP), Molecular Function (GOMF)[38] and Wikipathways[39]. Pathways at FDR < 0.05
291 were considered significant. Unless otherwise specified, R 3.5.2 was used for the
292 analysis mentioned in the RNA sequencing section.
293
294 **Additional Statistical methods**
295 Data are presented as means ± SEM. For analytic comparisons of body weight, total food
296 intake, and chow intake, groups were compared using repeated measures ANOVA in
297 Prism software (GraphPad Inc., version 8.0). Taxonomic comparisons from 16S rRNA
298 sequencing analysis were analyzed by analysis of composition of microbiomes
299 (ANCOM). When significant differences were detected, Sidak post-hoc test for multiple
300 comparisons was used. Area under the curve (AUC) for the IP GTT testing was also
301 calculated using Prism. All other statistical analyses were performed using Student's
302 two-tailed unpaired t tests in excel software (Microsoft Inc., version 15.26). Normality
303 was confirmed prior to the utilization of parametric testing. For all analyses, statistical
304 significance was set at $P<0.05$.
305
306 **<u>Results:</u>**

307 **Early-life sugar consumption impairs hippocampal-dependent memory**
308 **function**
309
310 Results from the Novel Object in Context (NOIC) task, which measures hippocampal-
311 dependent episodic contextual memory function [29], reveal that while there were no
312 differences in total exploration time of the combined objects on days 1 or 3 of the task
313 (Figure 1A, B), animals fed sugar solutions in early life beginning at PN 28 had a
314 reduced capacity to discriminate an object that was novel to a specific context when
315 animals were tested during adulthood (PN 60), indicating impaired hippocampal
316 function (Figure 1C). Conversely, animals fed sugar solutions in early life performed
317 similarly to those in the control group when tested in the novel object recognition task
318 (NOR) (Figure 1D), which tests object recognition memory independent of context.
319 Notably, when performed using the current methods with a short duration between the
320 familiarization phase and the test phase, NOR not hippocampal-dependent but instead
321 is primarily dependent on the perirhinal cortex [29, 40-42]. These data suggest that early life
322 dietary sugar consumption impairs performance in hippocampal-dependent contextual-
323 based recognition memory without affecting performance in perirhinal cortex-
324 dependent recognition memory independent of context [22].
325
326 Elevated anxiety-like behavior and altered general activity levels may influence novelty
327 exploration independent of memory effects and may therefore confound the
328 interpretation of behavioral results. Thus, we next tested whether early life sugar
329 consumption affects anxiety-like behavior using two different tasks designed to measure
330 anxiety-like behavior in the rat: the elevated zero maze and the open field task, that

331 latter of which also assesses levels of general activity [43]. Early life sugar consumption
332 had no effect on time spent in the open area or in the number of open area entries in the
333 zero maze (Figure 1E, F). Similarly, early life sugar had no effect on distance travelled or
334 time spent in the center zone in the open field task (Figure 1G, H). Together these data
335 suggest that habitual early life sugar consumption did not increase anxiety-like behavior
336 or general activity levels in the rats.
337

338 **Early life sugar consumption impairs glucose tolerance without affecting**
339 **total caloric intake, body weight, or adiposity**
340

341 Given that excessive sugar consumption is associated with weight gain and metabolic
342 deficits [44], we tested whether access to a sugar solution during the adolescent phase of
343 development would affect food intake, body weight gain, adiposity, and glucose
344 tolerance in the rat. Early life sugar consumption had no effect on body composition
345 during adulthood (Figure 1I, Figure S1 A, B). Early life sugar consumption also had no
346 effect on body weight or total kcal intake (Figure 1J, K), which is in agreement with
347 previous findings [22, 45, 46]. Animals steadily increased their intake of the 11% sugar
348 solution throughout the study (Figure 1L) but compensated for the calories consumed in
349 the sugar solutions by reducing their intake of dietary chow (Figure S1 C). However,
350 animals that were fed sugar solutions during adolescence showed impaired peripheral
351 glucose metabolism in an intraperitoneal glucose tolerance test (IP GTT) (Figure S1D).
352

353 **Gut microbiota are impacted by early life sugar consumption**
354

355 Principal component analyses of 16s rRNA gene sequencing data of fecal samples
356 revealed a separation between the fecal microbiota of rats fed early life sugar and
357 controls (Figure 2A). Results from LEfSe analysis identified differentially abundant
358 bacterial taxa in fecal samples that were elevated by sugar consumption. These include
359 the family *Clostridiaceae* and the genus *02d06* within *Clostridiaceae*, the family
360 *Mogibacteriaceae*, the family *Enterobacteriaceae*, the order *Enterobacteriales*, the
361 class of *Gammaproteobacteria*, and the genus *Parabacteroides* within the family
362 *Porphyromonadaceae* (Figure 2B,C). In addition to an elevated % relative abundance of
363 the genus *Parabacteroides* in animals fed early life sugar (Figure 2D), log transformed
364 counts of the *Parabacteroides* negatively correlated with performance scores in the
365 NOIC memory task (Figure 2E). Within *Parabacteroides*, levels of two operational
366 taxonomic units (OTUs) that were elevated by sugar negatively correlated with
367 performance in the NOIC task, identified as taxonomically related to *P. johnsonii* and *P.*
368 *distasonis* (Figure 2F, G). The significant negative correlation between NOIC
369 performance and *Parabacteroides* was also present within each of the diet groups alone,
370 but when separated out by diet group only *P. distasonis* showed a significant negative
371 correlation for each diet group ($P<.05$), whereas *P. johnsonii* showed a non-significant
372 trend in both the control and sugar groups ($P=.06$, and $P=.08$, respectively; Figure S2A-
373 C). Abundance of other bacterial populations that were affected by sugar consumption
374 were not significantly related to memory task performance.
375 There was a similar separation between groups in bacteria analyzed from cecal
376 samples (Figure S3A). LEfSe results from cecal samples show elevated *Bacilli*,
377 *Actinobacteria*, *Erysipelotrichia*, and *Gammaproteobacteria* in rats fed early life sugar,
378 and elevated *Clostridia* in the controls (Figure S3B-C). Abundances at the different

379 taxonomic levels in fecal and cecal samples are shown in (Figure S4, S5). Regression
380 analyses did not identify these altered cecal bacterial populations as being significantly
381 correlated to NOIC memory performance.
382
383 **Early life *Parabacteroides* enrichment impairs memory function**
384
385 To determine whether neurocognitive outcomes due to early life sugar consumption
386 could be attributable to elevated levels of *Parabacteroides* in the gut, we experimentally
387 enriched the gut microbiota of naïve juvenile rats with two *Parabacteroides* species that
388 exhibited high 16S rRNA sequencing alignment with OTUs that were increased by sugar
389 consumption and were negatively correlated with behavioral outcomes in rats fed early
390 life sugar. *P. johnsonii* and *P. distasoni* species were cultured individually under
391 anaerobic conditions and transferred to a group of antibiotic-treated young rats in a 1:1
392 ratio via oral gavage using the experimental design described in Methods and outlined
393 in Figure 3A, and from [27]. To confirm *Parabacteroides* enrichment, 16SrRNA
394 sequencing was performed on rat fecal samples for SAL-SAL, ABX-SAL, and ABX-PARA
395 groups. Alpha diversity was analyzed using observed operational taxonomic units
396 (OTUs) (Figure 3B), where both ABX-SAL and ABX-PARA fecal samples have
397 significantly reduced alpha diversity when compared with SAL-SAL fecal samples,
398 suggesting that antibiotic treatment reduces microbiome alpha diversity. Further, either
399 treatment with antibiotics alone or antibiotics followed by *Parabacteroides* significantly
400 alters microbiota composition relative to the SAL-SAL group (Figure 3C). Taxonomic
401 comparisons from 16S rRNA sequencing analysis were analyzed by analysis of
402 composition of microbiomes (ANCOM). Differential abundance on relative abundance

403 at the species level (Figure 3D) was tested across samples hypothesis-free. Significant
404 taxa at the species level were corrected for using false-discovery rate (FDR)-corrected *P*-
405 values to calculate W in ANCOM. Comparing all groups resulted in the highest W value
406 of 144 for the *Parabacteroides* genus, which was enriched in ABX-PARA fecal samples
407 after bacterial gavage with an average relative abundance of 55.65% (Figure 3E). This
408 confirms successful *Parabacteroides* enrichment for ABX-PARA rats post-gavage when
409 compared to either ABX-SAL (average relative abundance of 5.47%) or ABX-SAL rats
410 (average relative abundance of 0.26%).

411 All rats treated with antibiotics showed a reduction in food intake and body
412 weight during the initial stages of antibiotic treatment, however, there were no
413 differences in body weight between the two groups of antibiotic treated animals by
414 PN50, at the time of behavioral testing (Figure S6A-C). Similar to a recent report [47],
415 *Parabacteroides* enrichment in the present study impacted body weight at later time
416 points. Animals who received *P. johnsonii* and *P. distasonis* treatment showed reduced
417 body weight 40 days after the transfer, with significantly lower lean mass (Figure S6D-
418 F). There were no differences in percent body fat between groups, nor were there
419 significant group differences in glucose metabolism in the IPGTT (Figure S6 G).
420 Importantly, the body weights in the ABX-PARA group did not significantly differ from
421 the ABX-SAL control group at the time of behavioral testing.

422 Results from the hippocampal-dependent NOIC memory task showed that while
423 there were no differences in total exploration time of the combined objects on days 1 or
424 3 of the task, indicating similar exploratory behavior, animals enriched with
425 *Parabacteroides* showed a significantly reduced discrimination index in the NOIC task
426 compared with either control group (Figure 4A-C), indicating impaired performance in

427 hippocampal-dependent memory function. When tested in the perirhinal cortex-
428 dependent NOR task [29], animals enriched with *Parabacteroides* showed impaired object
429 recognition memory compared with the antibiotic treated control group as indicated by
430 a reduced novel object exploration index (Figure 4D). These findings show that unlike
431 sugar-fed animals, *Parabacteroides* enrichment impaired perirhinal cortex-dependent
432 memory processes in addition to hippocampal-dependent memory.

433 Results from the zero maze showed no differences in time spent in the open arms
434 nor in the number of open arm entries for the *Parabacteroides*-enriched rats relative to
435 controls (Figure 4E, F), indicating that the enrichment did not affect anxiety-like
436 behavior. Similarly, there were no differences in distance travelled or time spent in the
437 center arena in the open field test, which is a measure of both anxiety-like behavior and
438 general activity in rodents (Figure 4G, H). Together these data suggest that
439 *Parabacteroides* treatment negatively impacted both hippocampal-dependent
440 perirhinal cortex-dependent memory function without significantly affecting general
441 activity or anxiety-like behavior.

442

443 **Early life sugar consumption and *Parabacteroides* enrichment alter**
444 **hippocampal gene expression profiles**

445

446 To further investigate how sugar and *Parabacteroides* affect cognitive behaviors, we
447 conducted transcriptome analysis of the hippocampus samples. Figure S7 (A, C) shows
448 the results of principal component analysis revealing moderate separation based on
449 RNA sequencing data from the dorsal hippocampus of rats fed sugar in early life
450 compared with controls. Gene pathway enrichment analyses from RNA sequencing data

451 revealed multiple pathways significantly affected by early life sugar consumption,
452 including four pathways involved in neurotransmitter synaptic signaling: dopaminergic,
453 glutamatergic, cholinergic, and serotonergic signaling pathways. Additionally, several
454 gene pathways that also varied by sugar were those involved in kinase-mediated
455 intracellular signaling: cGMP-PKG, RAS, cAMP, and MAPK signaling pathways (Figure
456 5A, Table S1).

457 Analyses of individual genes across the entire transcriptome using a stringent
458 false-discovery rate criterion further identified 21 genes that were differentially
459 expressed in rats fed early life sugar compared with controls, with 11 genes elevated and
460 10 genes decreased in rats fed sugar compared to controls (Figure 5B). Among the genes
461 impacted, several genes that regulate cell survival, migration, differentiation, and DNA
462 repair were elevated by early life sugar access, including *Faap100*, which encodes an FA
463 core complex member of the DNA damage response pathway [48], and *Eepd1*, which
464 transcribes an endonuclease involved in repairing stalled DNA replication forks,
465 stressed from DNA damage [49]. Other genes associated with endoplasmic reticulum
466 stress and synaptogenesis were also significantly increased by sugar consumption,
467 including *Klf9, Dgkh, Neurod2, Ppl*, and *Kirrel1* [50,51,52,53].

468 Several genes were reduced by dietary sugar, including *Tns2*, which encodes
469 tensin 2, important for cell migration [54], *RelA*, which encodes a NF/kB complex protein
470 that regulates activity dependent neuronal function and synaptic plasticity [55], and
471 *Grm8*, the gene for the metabotropic glutamate receptor 8 (mGluR8). Notably, reduced
472 expression of mGluR8 receptor may contribute to the impaired neurocognitive
473 functioning in animals fed sugar, as mGluR8 knockout mice show impaired
474 hippocampal-dependent learning and memory [56].

475 Figure S7 (A-B, D) shows the results of principal component analysis of dorsal
476 hippocampus RNA sequencing data indicating moderate separation between rats
477 enriched with *Parabacteroides* and controls. Gene pathway analyses revealed that early
478 life *Parabacteroides* treatment, similar to effects associated with sugar consumption,
479 significantly altered the genetic signature of dopaminergic synaptic signaling pathways,
480 though differentially expressed genes were commonly affected in opposite directions
481 between the two experimental conditions (Figure S8). *Parabacteroides* treatment also
482 impacted gene pathways associated with metabolic signaling. Specifically, pathways
483 regulating fatty acid oxidation, rRNA metabolic processes, mitochondrial inner
484 membrane, and valine, leucine, and isoleucine degradation were significantly affected by
485 *Parabacteroides* enrichment. Other pathways that were influenced were those involved
486 in neurodegenerative disorders, including Alzheimer's disease and Parkinson's disease,
487 though most of the genes affected in these pathways were mitochondrial genes (Figure
488 5D, Table S2).
489 At the level of individual genes, dorsal hippocampal RNA sequencing data
490 revealed that 15 genes were differentially expressed in rats enriched with
491 *Parabacteroides* compared with controls, with 13 genes elevated and two genes
492 decreased in the *Parabacteroides* group compared with controls (Figure 6C). Consistent
493 with results from gene pathway analyses, several individual genes involved in metabolic
494 processes were elevated by *Parabacteroides* enrichment, such as *Hmgcs2*, which is a
495 mitochondrial regulator of ketogenesis and provides energy to the brain under
496 metabolically taxing conditions or when glucose availability is low [57], and *Cox6b1*, a
497 mitochondrial regulator of energy metabolism that improves hippocampal cellular
498 viability following ischemia/reperfusion injury [58]. *Parabacteroides* enrichment was also

499 associated with incased expression of *Slc27A1* and *Mfrp*, which are each critical for the
500 transport of fatty acids into the brain across capillary endothelial cells [59,60].
501
502 **Discussion:**
503 Dietary factors are a key source of gut microbiome diversity [27, 45, 61-63] and
504 emerging evidence indicates that diet-induced alterations in the gut microbiota may be
505 linked with altered neurocognitive development [27, 63-65]. Our results identify species
506 within the genus *Parabacteroides* that are elevated by habitual early life consumption of
507 dietary sugar and are negatively associated with hippocampal-dependent memory
508 performance. Further, targeted microbiota enrichment of *Parabacteroides* perturbed
509 both hippocampal- and perirhinal cortex-dependent memory performance. These
510 findings are consistent with previous literature in showing that early life consumption of
511 Western dietary factors impair neurocognitive outcomes [8, 9], and further suggest that
512 altered gut bacteria due to excessive early life sugar consumption may functionally link
513 dietary patterns with cognitive impairment.
514 Our previous data show that rats are not susceptible to habitual sugar
515 consumption-induced learning and memory impairments when 11% sugar solutions are
516 consumed ad libitum during adulthood, in contrast to effects observed in the present
517 and previous study in which the sugar is consumed during early life development [22]. It is
518 possible that habitual sugar consumption differentially affects the gut microbiome when
519 consumed during adolescence vs. adulthood. However, a recent report showed that
520 adult consumption of a high fructose diet (35% kcal from fructose) promotes gut
521 microbial "dysbiosis" and neuroinflammation and cell death in the hippocampus, yet
522 without impacting cognitive function [66], suggesting that perhaps neurocognitive

523 function is more susceptible to gut microbiota influences during early life than during
524 adulthood. Indeed, several reports have identified early life critical periods for
525 microbiota influences on behavioral and neurochemical endpoints in germ free mice [3, 5
526 4]. However, the age-specific profile of sugar-associated microbiome dysbiosis and
527 neurocognitive impairments remains to be determined.

528 While our study reveals a strong negative correlation between levels of fecal
529 *Parabacteroides* and performance in the hippocampal-dependent contextual episodic
530 memory NOIC task, as well as impaired NOIC performance in rats given access to a
531 sugar solution during adolescence, sugar intake did not produce impairments in the
532 perirhinal cortex-dependent NOR memory task. That early life sugar consumption
533 negatively impacts hippocampal-dependent spatial [22] and contextual-based learning
534 without influencing NOR performance is consistent with previous reports using a
535 cafeteria diet high in both fat content and sugar [67, 68]. On the other hand, enrichment of
536 *P. johnsonii* and *P. distasonis* in the present study impaired memory performance in
537 both tasks, suggesting a broader impact on neurocognitive functioning with this
538 targeted bacterial enrichment approach.

539 Gene pathway analyses from dorsal hippocampus RNA sequencing identified
540 multiple neurobiological pathways that may functionally connect gut dysbiosis with
541 memory impairment. Early life sugar consumption was associated with alterations in
542 several neurotransmitter synaptic signaling pathways (e.g., glutamatergic, cholinergic)
543 and intracellular signaling targets (e.g., cAMP, MAPK). A different profile was observed
544 in *Parabacteroides*-enriched animals, where gene pathways involved with metabolic
545 function (e.g., fatty acid oxidation, branched chain amino acid degradation) and
546 neurodegenerative disease (e.g., Alzheimer's disease) were altered relative to controls.

547 Given that sugar has effects on bacterial populations in addition to *Parabacteroides*,
548 and that sugar consumption and *Parabacteroides* treatment differentially influenced
549 peripheral glucose metabolism and body weight, these transcriptome differences in the
550 hippocampus are not surprising. However, gene clusters involved with dopaminergic
551 synaptic signaling were significantly influenced by both early life sugar consumption
552 and *Parabacteroides* treatment, thus identifying a common pathway through which
553 both diet-induced and gut bacterial infusion-based elevations in *Parabacteroides* may
554 influence neurocognitive development. Though differentially expressed genes were
555 commonly affected in opposite directions in *Parabacteroides* enriched animals
556 compared with early life sugar treated animals, it is possible that perturbations to the
557 dopamine system play a role in the observed cognitive dysfunction. For example, while
558 dopamine signaling in the hippocampus has not traditionally been investigated for
559 mediating memory processes, several recent reports have identified a role for dopamine
560 inputs from the locus coeruleus in regulating hippocampal-dependent memory and
561 neuronal activity [69, 70]. Interestingly, endogenous dopamine signaling in the
562 hippocampus has recently been linked with regulating food intake and food-associated
563 contextual learning [71], suggesting that dietary effects on gut microbiota may also impact
564 feeding behavior and energy balance-relevant cognitive processes.
565 Many of the genes that were differentially upregulated in the hippocampus by
566 *Parabacteroides* enrichment were involved in fat metabolism and transport. Thus, it is
567 possible that *Parabacteroides* conferred an adaptation in the brain, shifting fuel
568 preference away from carbohydrate toward lipid-derived ketones. Consistent with this
569 framework, *Parabacteroides* was previously shown to be upregulated by a ketogenic
570 diet in which carbohydrate consumption is drastically depleted and fat is used as a

571 primary fuel source due. Furthermore, enrichment of *Parabacteroides merdae* together
572 with *Akkermansia muciniphila* was protective against seizures in mice [27]. It is possible
573 that *P. distasonis* reduces glucose uptake from the gut, enhances glucose clearing from
574 the blood, and/or alters nutrient utilization in general, an idea further supported by
575 recent finding that *P. distasonis* is associated with reduced diet- and genetic-induced
576 obesity and hyperglycemia in mice [47].

577 Collective results provide mechanistic insight into the neurobiological
578 mechanisms that link early life unhealthy dietary patters with altered gut microbiota
579 changes and neurocognitive impairments. Currently probiotics, live microorganisms
580 intended to confer health benefits, are not regulated with the same rigor as
581 pharmaceuticals but instead are sold as dietary supplements. Our findings suggest that
582 gut enrichment with certain species of *Parabacteroides* is potentially harmful for
583 neurocognitive mnemonic development. These results highlight the importance of
584 conducting rigorous basic science analyses on the relationship between diet,
585 microorganisms, brain, and behavior prior to widespread recommendations of bacterial
586 microbiome interventions for humans.

587

588 **Acknowledgements:**

589 We thank Alyssa Cortella for contributing the rodent artwork. We thank Caroline
590 Szjewski, Lekha Chirala, Vaibhav Konanur, Sarah Terrill, and Ted Hsu for their critical
591 contributions to the research. The research was supported by DK116942, DK104897,
592 and institutional funds to S.E.K., DK111158 to E.E.N., DK116558 to A.N.S., DK 118944 to
593 C.M.L. C.A.O. was supported by an F31 AG064844. E.Y.H. was supported by ARO

MURI award W911NF-17-1-0402. DK104363 to X.Y., Eureka Scholarship and BWF-CHIP Fellowship to Y.C.

Author Contributions:

E.E.N., E.Y.H., and S.E.K. designed the experiments. E.E.N. performed the majority of the behavioral experiments and analyzed the data. C.A.O. and E.Y.H. contributed to the design and implementation of the bacterial enrichment procedure, quantified *Parabacteroides* enrichment, and helped with data analyses. E.D. helped with the behavioral experiments and performed the RNA sequencing preparation with Y.C. and X.Y. for analyses of the RNA sequencing data. R.J., M.G., R. S. and C.D.L.S., performed the gut microbiome analyses. L.T., C.L., and A.S., helped with behavioral experiments. The paper was written by E.E.N and S.E.K. with additional editorial input from the other authors.

Conflicts of Interest:

The authors declare no competing interests

References:

1. Vuong HE, Yano JM, Fung TC, Hsiao EY. The Microbiome and Host Behavior. *Annu Rev Neurosci* 2017; **40:** 21-49.

2. Noble EE, Hsu TM, Kanoski SE. Gut to Brain Dysbiosis: Mechanisms Linking Western Diet Consumption, the Microbiome, and Cognitive Impairment. *Front Behav Neurosci* 2017; **11:** 9.

3. Neufeld KA, Kang N, Bienenstock J, Foster JA. Effects of intestinal microbiota on anxiety-like behavior. *Commun Integr Biol* 2011; **4**(4)**:** 492-494.

4. Sudo N, Chida Y, Aiba Y, Sonoda J, Oyama N, Yu XN *et al.* Postnatal microbial colonization programs the hypothalamic-pituitary-adrenal system for stress response in mice. *J Physiol* 2004; **558**(Pt 1)**:** 263-275.

5. Diaz Heijtz R, Wang S, Anuar F, Qian Y, Bjorkholm B, Samuelsson A *et al.* Normal gut microbiota modulates brain development and behavior. *Proc Natl Acad Sci U S A* 2011; **108**(7)**:** 3047-3052.

6. Cryan JF, O'Riordan KJ, Cowan CSM, Sandhu KV, Bastiaanssen TFS, Boehme M *et al.* The Microbiota-Gut-Brain Axis. *Physiological reviews* 2019; **99**(4)**:** 1877-2013.

7. Kanoski SE, Davidson TL. Western diet consumption and cognitive impairment: links to hippocampal dysfunction and obesity. *Physiol Behav* 2011; **103**(1)**:** 59-68.

8. Noble EE, Hsu TM, Liang J, Kanoski SE. Early-life sugar consumption has long-term negative effects on memory function in male rats. *Nutritional neuroscience* 2019**:** 1-11.

9. Noble EE, Kanoski SE. Early life exposure to obesogenic diets and learning and memory dysfunction. *Curr Opin Behav Sci* 2016; **9:** 7-14.

10. Hsu TM, Noble EE, Reiner DJ, Liu CM, Suarez AN, Konanur VR *et al.* Hippocampus ghrelin receptor signaling promotes socially-mediated learned food preference. *Neuropharmacology* 2018; **131:** 487-496.

11. Hsu TM, Noble EE, Liu CM, Cortella AM, Konanur VR, Suarez AN *et al.* A hippocampus to prefrontal cortex neural pathway inhibits food motivation through glucagon-like peptide-1 signaling. *Mol Psychiatry* 2018; **23**(7)**:** 1555-1565.

12. Hsu TM, Hahn JD, Konanur VR, Noble EE, Suarez AN, Thai J *et al.* Hippocampus ghrelin signaling mediates appetite through lateral hypothalamic orexin pathways. *Elife* 2015; **4**.

652 13. Kanoski SE, Fortin SM, Ricks KM, Grill HJ. Ghrelin signaling in the ventral hippocampus
653 stimulates learned and motivational aspects of feeding via PI3K-Akt signaling. *Biol*
654 *Psychiatry* 2013; **73**(9)**:** 915-923.
655
656 14. Davidson TL, Chan K, Jarrard LE, Kanoski SE, Clegg DJ, Benoit SC. Contributions of the
657 hippocampus and medial prefrontal cortex to energy and body weight regulation.
658 *Hippocampus* 2009; **19**(3)**:** 235-252.
659
660 15. Kanoski SE, Grill HJ. Hippocampus Contributions to Food Intake Control: Mnemonic,
661 Neuroanatomical, and Endocrine Mechanisms. *Biol Psychiatry* 2017; **81**(9)**:** 748-756.
662
663 16. Kanoski SE, Davidson TL. Western diet consumption and cognitive impairment: links to
664 hippocampal dysfunction and obesity. *Physiol Behav* 2011; **103**(1)**:** 59-68.
665
666 17. Davidson TL, Sample CH, Swithers SE. An application of Pavlovian principles to the
667 problems of obesity and cognitive decline. *Neurobiology of learning and memory* 2014;
668 **108:** 172-184.
669
670 18. Baym CL, Khan NA, Monti JM, Raine LB, Drollette ES, Moore RD *et al.* Dietary lipids are
671 differentially associated with hippocampal-dependent relational memory in
672 prepubescent children. *Am J Clin Nutr* 2014; **99**(5)**:** 1026-1032.
673
674 19. Valladolid-Acebes I, Fole A, Martin M, Morales L, Cano MV, Ruiz-Gayo M *et al.* Spatial
675 memory impairment and changes in hippocampal morphology are triggered by high-fat
676 diets in adolescent mice. Is there a role of leptin? *Neurobiol Learn Mem* 2013; **106:** 18-
677 25.
678
679 20. Boitard C, Cavaroc A, Sauvant J, Aubert A, Castanon N, Laye S *et al.* Impairment of
680 hippocampal-dependent memory induced by juvenile high-fat diet intake is associated
681 with enhanced hippocampal inflammation in rats. *Brain Behav Immun* 2014; **40:** 9-17.
682
683 21. Boitard C, Etchamendy N, Sauvant J, Aubert A, Tronel S, Marighetto A *et al.* Juvenile, but
684 not adult exposure to high-fat diet impairs relational memory and hippocampal
685 neurogenesis in mice. *Hippocampus* 2012; **22**(11)**:** 2095-2100.
686
687 22. Hsu TM, Konanur VR, Taing L, Usui R, Kayser BD, Goran MI *et al.* Effects of sucrose and
688 high fructose corn syrup consumption on spatial memory function and hippocampal
689 neuroinflammation in adolescent rats. *Hippocampus* 2015; **25**(2)**:** 227-239.
690
691 23. Kendig MD, Boakes RA, Rooney KB, Corbit LH. Chronic restricted access to 10% sucrose
692 solution in adolescent and young adult rats impairs spatial memory and alters sensitivity
693 to outcome devaluation. *Physiol Behav* 2013; **120:** 164-172.
694

24. Reichelt AC, Killcross S, Hambly LD, Morris MJ, Westbrook RF. Impact of adolescent sucrose access on cognitive control, recognition memory, and parvalbumin immunoreactivity. *Learn Mem* 2015; **22**(4)**:** 215-224.

25. Noble EE, Hsu TM, Liang J, Kanoski SE. Early-life sugar consumption has long-term negative effects on memory function in male rats. *Nutr Neurosci* 2019; **22**(4)**:** 273-283.

26. Walker RW, Dumke KA, Goran MI. Fructose content in popular beverages made with and without high-fructose corn syrup. *Nutrition* 2014; **30**(7-8)**:** 928-935.

27. Olson CA, Vuong HE, Yano JM, Liang QY, Nusbaum DJ, Hsiao EY. The Gut Microbiota Mediates the Anti-Seizure Effects of the Ketogenic Diet. *Cell* 2018; **173**(7)**:** 1728-1741 e1713.

28. Martinez MC, Villar ME, Ballarini F, Viola H. Retroactive interference of object-in-context long-term memory: role of dorsal hippocampus and medial prefrontal cortex. *Hippocampus* 2014; **24**(12)**:** 1482-1492.

29. Balderas I, Rodriguez-Ortiz CJ, Salgado-Tonda P, Chavez-Hurtado J, McGaugh JL, Bermudez-Rattoni F. The consolidation of object and context recognition memory involve different regions of the temporal lobe. *Learn Mem* 2008; **15**(9)**:** 618-624.

30. Beilharz JE, Maniam J, Morris MJ. Short exposure to a diet rich in both fat and sugar or sugar alone impairs place, but not object recognition memory in rats. *Brain Behav Immun* 2014; **37:** 134-141.

31. Thompson LR, Sanders JG, McDonald D, Amir A, Ladau J, Locey KJ *et al.* A communal catalogue reveals Earth's multiscale microbial diversity. *Nature* 2017; **551**(7681)**:** 457-463.

32. Caporaso JG, Lauber CL, Walters WA, Berg-Lyons D, Huntley J, Fierer N *et al.* Ultra-high-throughput microbial community analysis on the Illumina HiSeq and MiSeq platforms. *ISME J* 2012; **6**(8)**:** 1621-1624.

33. Patro R, Duggal G, Love MI, Irizarry RA, Kingsford C. Salmon provides fast and bias-aware quantification of transcript expression. *Nat Methods* 2017; **14**(4)**:** 417-419.

34. Soneson C, Love MI, Robinson MD. Differential analyses for RNA-seq: transcript-level estimates improve gene-level inferences. *F1000Res* 2015; **4:** 1521.

35. Anders S, Huber W. Differential expression analysis for sequence count data. *Genome Biol* 2010; **11**(10)**:** R106.

36. Kuleshov MV, Jones MR, Rouillard AD, Fernandez NF, Duan Q, Wang Z *et al.* Enrichr: a comprehensive gene set enrichment analysis web server 2016 update. *Nucleic Acids Res* 2016; **44**(W1)**:** W90-97.

37. Kanehisa M, Furumichi M, Tanabe M, Sato Y, Morishima K. KEGG: new perspectives on genomes, pathways, diseases and drugs. *Nucleic Acids Res* 2017; **45**(D1)**:** D353-D361.

38. The Gene Ontology C. Expansion of the Gene Ontology knowledgebase and resources. *Nucleic Acids Res* 2017; **45**(D1)**:** D331-D338.

39. Slenter DN, Kutmon M, Hanspers K, Riutta A, Windsor J, Nunes N *et al.* WikiPathways: a multifaceted pathway database bridging metabolomics to other omics research. *Nucleic Acids Res* 2018; **46**(D1)**:** D661-D667.

40. Aggleton JP, Brown MW. Contrasting hippocampal and perirhinal cortex function using immediate early gene imaging. *Q J Exp Psychol B* 2005; **58**(3-4)**:** 218-233.

41. Albasser MM, Davies M, Futter JE, Aggleton JP. Magnitude of the object recognition deficit associated with perirhinal cortex damage in rats: Effects of varying the lesion extent and the duration of the sample period. *Behav Neurosci* 2009; **123**(1)**:** 115-124.

42. Cohen SJ, Stackman RW, Jr. Assessing rodent hippocampal involvement in the novel object recognition task. A review. *Behav Brain Res* 2015; **285:** 105-117.

43. Sestakova N, Puzserova A, Kluknavsky M, Bernatova I. Determination of motor activity and anxiety-related behaviour in rodents: methodological aspects and role of nitric oxide. *Interdiscip Toxicol* 2013; **6**(3)**:** 126-135.

44. Goran MI, Dumke K, Bouret SG, Kayser B, Walker RW, Blumberg B. The obesogenic effect of high fructose exposure during early development. *Nat Rev Endocrinol* 2013; **9**(8)**:** 494-500.

45. Noble EE, Hsu TM, Jones RB, Fodor AA, Goran MI, Kanoski SE. Early-Life Sugar Consumption Affects the Rat Microbiome Independently of Obesity. *J Nutr* 2017; **147**(1)**:** 20-28.

46. Noble EE, Hsu TM, Liang J, Kanoski SE. Early-life sugar consumption has long-term negative effects on memory function in male rats. *Nutr Neurosci* 2017**:** 1-11.

47. Wang K, Liao M, Zhou N, Bao L, Ma K, Zheng Z *et al.* Parabacteroides distasonis Alleviates Obesity and Metabolic Dysfunctions via Production of Succinate and Secondary Bile Acids. *Cell Rep* 2019; **26**(1)**:** 222-235 e225.

781 48. Ling C, Ishiai M, Ali AM, Medhurst AL, Neveling K, Kalb R *et al.* FAAP100 is essential for
782 activation of the Fanconi anemia-associated DNA damage response pathway. *EMBO J*
783 2007; **26**(8)**:** 2104-2114.
784
785 49. Kim HS, Nickoloff JA, Wu Y, Williamson EA, Sidhu GS, Reinert BL *et al.* Endonuclease
786 EEPD1 Is a Gatekeeper for Repair of Stressed Replication Forks. *J Biol Chem* 2017;
787 **292**(7)**:** 2795-2804.
788
789 50. Zucker SN, Fink EE, Bagati A, Mannava S, Bianchi-Smiraglia A, Bogner PN *et al.* Nrf2
790 amplifies oxidative stress via induction of Klf9. *Mol Cell* 2014; **53**(6)**:** 916-928.
791
792 51. Yasuda S, Kai M, Imai S, Takeishi K, Taketomi A, Toyota M *et al.* Diacylglycerol kinase eta
793 augments C-Raf activity and B-Raf/C-Raf heterodimerization. *J Biol Chem* 2009; **284**(43)**:**
794 29559-29570.
795
796 52. Murdoch H, Feng GJ, Bachner D, Ormiston L, White JH, Richter D *et al.* Periplakin
797 interferes with G protein activation by the melanin-concentrating hormone receptor-1
798 by binding to the proximal segment of the receptor C-terminal tail. *J Biol Chem* 2005;
799 **280**(9)**:** 8208-8220.
800
801 53. Gerke P, Benzing T, Hohne M, Kispert A, Frotscher M, Walz G *et al.* Neuronal expression
802 and interaction with the synaptic protein CASK suggest a role for Neph1 and Neph2 in
803 synaptogenesis. *J Comp Neurol* 2006; **498**(4)**:** 466-475.
804
805 54. Chen H, Duncan IC, Bozorgchami H, Lo SH. Tensin1 and a previously undocumented
806 family member, tensin2, positively regulate cell migration. *Proc Natl Acad Sci U S A*
807 2002; **99**(2)**:** 733-738.
808
809 55. O'Mahony A, Raber J, Montano M, Foehr E, Han V, Lu SM *et al.* NF-kappaB/Rel regulates
810 inhibitory and excitatory neuronal function and synaptic plasticity. *Mol Cell Biol* 2006;
811 **26**(19)**:** 7283-7298.
812
813 56. Gerlai R, Adams B, Fitch T, Chaney S, Baez M. Performance deficits of mGluR8 knockout
814 mice in learning tasks: the effects of null mutation and the background genotype.
815 *Neuropharmacology* 2002; **43**(2)**:** 235-249.
816
817 57. Shao X, Tang Y, Long H, Gu H, Zhang J, Deng P *et al.* HMG-CoA synthase 2 drives brain
818 metabolic reprogramming in cocaine exposure. *Neuropharmacology* 2019; **148:** 377-
819 393.
820
821 58. Yang S, Wu P, Xiao J, Jiang L. Overexpression of COX6B1 protects against I/Rinduced
822 neuronal injury in rat hippocampal neurons. *Mol Med Rep* 2019; **19**(6)**:** 4852-4862.
823

59. Ochiai Y, Uchida Y, Ohtsuki S, Tachikawa M, Aizawa S, Terasaki T. The blood-brain barrier fatty acid transport protein 1 (FATP1/SLC27A1) supplies docosahexaenoic acid to the brain, and insulin facilitates transport. *J Neurochem* 2017; **141**(3)**:** 400-412.

60. Kautzmann MI, Gordon WC, Jun B, Do KV, Matherne BJ, Fang Z *et al.* Membrane-type frizzled-related protein regulates lipidome and transcription for photoreceptor function. *FASEB J* 2020; **34**(1)**:** 912-929.

61. David LA, Maurice CF, Carmody RN, Gootenberg DB, Button JE, Wolfe BE *et al.* Diet rapidly and reproducibly alters the human gut microbiome. *Nature* 2014; **505**(7484)**:** 559-563.

62. de La Serre CB, Ellis CL, Lee J, Hartman AL, Rutledge JC, Raybould HE. Propensity to high-fat diet-induced obesity in rats is associated with changes in the gut microbiota and gut inflammation. *Am J Physiol Gastrointest Liver Physiol* 2010; **299**(2)**:** G440-448.

63. Bruce-Keller AJ, Salbaum JM, Luo M, Blanchard Et, Taylor CM, Welsh DA *et al.* Obese-type gut microbiota induce neurobehavioral changes in the absence of obesity. *Biol Psychiatry* 2015; **77**(7)**:** 607-615.

64. Leigh SJ, Kaakoush NO, Westbrook RF, Morris MJ. Minocycline-induced microbiome alterations predict cafeteria diet-induced spatial recognition memory impairments in rats. *Transl Psychiatry* 2020; **10**(1)**:** 92.

65. Leigh SJ, Kaakoush NO, Bertoldo MJ, Westbrook RF, Morris MJ. Intermittent cafeteria diet identifies fecal microbiome changes as a predictor of spatial recognition memory impairment in female rats. *Transl Psychiatry* 2020; **10**(1)**:** 36.

66. Li JM, Yu R, Zhang LP, Wen SY, Wang SJ, Zhang XY *et al.* Dietary fructose-induced gut dysbiosis promotes mouse hippocampal neuroinflammation: a benefit of short-chain fatty acids. *Microbiome* 2019; **7**(1)**:** 98.

67. Kendig MD, Westbrook RF, Morris MJ. Pattern of access to cafeteria-style diet determines fat mass and degree of spatial memory impairments in rats. *Sci Rep* 2019; **9**(1)**:** 13516.

68. Yang Y, Zhong Z, Wang B, Xia X, Yao W, Huang L *et al.* Early-life high-fat diet-induced obesity programs hippocampal development and cognitive functions via regulation of gut commensal Akkermansia muciniphila. *Neuropsychopharmacology* 2019; **44**(12)**:** 2054-2064.

69. Takeuchi T, Duszkiewicz AJ, Sonneborn A, Spooner PA, Yamasaki M, Watanabe M *et al.* Locus coeruleus and dopaminergic consolidation of everyday memory. *Nature* 2016; **537**(7620)**:** 357-362.

70. Kempadoo KA, Mosharov EV, Choi SJ, Sulzer D, Kandel ER. Dopamine release from the locus coeruleus to the dorsal hippocampus promotes spatial learning and memory. *Proc Natl Acad Sci U S A* 2016; **113**(51)**:** 14835-14840.

71. Azevedo EP, Pomeranz L, Cheng J, Schneeberger M, Vaughan R, Stern SA *et al.* A Role of Drd2 Hippocampal Neurons in Context-Dependent Food Intake. *Neuron* 2019; **102**(4)**:** 873-886 e875.

879 **Figure Legends:**

880

881 **Figure 1: Early-life sugar consumption negatively impacts hippocampal-**
882 **dependent memory function.** (A, B) Early life sugar consumption had no effect on
883 total exploration time on days 1 (familiarization) or day 3 (test day) of the Novel Object
884 in Context (NOIC) task. (C) The discrimination index was significantly reduced by early
885 life sugar consumption, indicating impaired hippocampal function (P<.05, n=10,11;
886 two-tailed, type 2 Student's T-test). (D) There were no differences in exploration index
887 in the Novel Object Recognition (NOR task) (n=6; two-tailed, type 2 Student's T-test).
888 (E, F) There were no differences in time spent in the open arm or the number of entries
889 into the open arm in the Zero Maze task for anxiety-like behavior (n=10; two-tailed, type
890 2 Student's t-test). (G, H) There were no differences in distance travelled or time spent
891 in the center arena in the Open Field task (n=8; two-tailed, type 2 Student's T-test). (I)
892 There were no differences in body fat % during adulthood between rats fed early life
893 sugar and controls (n=10,11; two-tailed, type 2 Student's T-test). (J-K) Body weights and
894 total energy intake did not differ between the groups (n=10,11; two- way repeated
895 measures ANOVA), despite (L) increased kcal consumption from sugar sweetened
896 beverages in the sugar group. CTL=control, SUG= sugar, PN= post-natal day; data
897 shown as mean ± SEM.

898

899 **Figure 2: Effect of adolescent sugar consumption on the gut microbiome in**
900 **rats.** (A) Principal component analysis showing separation between fecal microbiota of
901 rats fed early life sugar or controls (n=11, 10; dark triangles= sugar, open circles=
902 control). (B) Results from LEfSe analysis showing Linear Discriminate Analysis (LDA)

903 scores for microbiome analysis of fecal samples of rats fed early life sugar or controls.
904 (C) A cladogram representing the results from the LEfSe analysis with class as the outer
905 most taxonomic level and species at the inner most level. Taxa in red are elevated in the
906 sugar group. (D) Relative % abundance of fecal *Parabacteroides* are significantly
907 elevated in rats fed early life sugar (P<.05; n=11, 10, two-tailed, type 2 Student's T-test).
908 (E) Linear regression of log normalized fecal *Parabacteroides* counts against shift from
909 baseline performance scores in the novel object in context task (NOIC) across all groups
910 tested (n=21). (E, F) Linear regression of the most abundant fecal *Parabacteroides*
911 species against shift from baseline performance scores in NOIC across all groups tested
912 (n=21). *P<0.05; data shown as mean ± SEM.
913
914 **Figure 3: Intestinal *Parabacteroides* is enriched by antibiotic treatment**
915 **and oral gavage of *P. distasonis* and *P. johnsonii*.** A) Schematic showing the
916 timeline for the experimental design of the *Parabacteroides* transfer experiment. B)
917 Alpha diversity based on 16S rRNA gene profiling of fecal matter (n=7-8) represented by
918 observed operational taxonomic units (OTUs) for a given number of sample sequences.
919 C) Principal coordinates analysis of weighted UniFrac distance based on 16S rRNA gene
920 profiling of feces for SAL-SAL, ABX-SAL, and ABX-PARA enriched rats (n=7-8). D)
921 Average taxonomic distributions of bacteria from 16S rRNA gene sequencing data of
922 feces for SAL-SAL, ABX-SAL, and ABX-PARA enriched animals (n=7-8). E) Relative
923 abundances of *Parabacteroides* in fecal microbiota for SAL-SAL, ABX-SAL, and ABX-
924 PARA enriched animals (n=7-8) (ANCOM). PN= post-natal day, IP GTT=
925 intraperitoneal glucose tolerance test. Data are presented as mean ± S.E.M. * $p < 0.05$,
926 ** $p < 0.01$, *** $p < 0.001$. n.s.=not statistically significant. SAL-SAL= rats treated with

927 saline, ABX-SAL=rats treated with antibiotics followed by sterile saline gavage, ABX-
928 PARA= rats treated with antibiotics followed by a 1:1 gavage of *Parabacteroides*
929 *distasonis* and *Parabacteroides johnsonii*.
930
931 **Figure 4: Early-life enrichment with *Parabacteroides* negatively impacts**
932 **neurocognitive function.** (A, B) Early-life enrichment with a 1:1 ratio of *P. johnsonii*
933 and *P. distasonis* had no effect on total exploration time in the Novel Object in Context
934 (NOIC) task. (C) Discrimination index was significantly reduced by enrichment with *P.*
935 *johnsonii* and *P. distasonis*, indicating impaired hippocampal function (n=7,8; $F_{(2, 19)}$ =
936 4.92; P< .05, one-way ANOVA with Tukey's multiple comparison test). (D) There was a
937 significant reduction in the exploration index in the Novel Object Recognition (NOR
938 task), indicating impaired perirhinal cortex function (n=7,8; $F_{(2, 19)}$ = 3.61; P< .05, one-
939 way ANOVA with Tukey's multiple comparison test). (E, F) There were no differences in
940 time spent or number of entries into the open arm by animals with *P. johnsonii* and *P.*
941 *distasonis* enrichment in the Zero Maze task for anxiety-like behavior (n=7,8; one-way
942 ANOVA) . (G, H) There were no differences in distance travelled or time spent in the
943 center arena in the Open Field task (n=7,8; one-way ANOVA). SAL-SAL=saline-saline
944 control, ABX-SAL= antibiotics-saline control, ABX-PARA= antibiotics-*P. johnsonii* and
945 *P. distasonis* enriched, PN= post-natal day; data shown as mean ± SEM; * *P*<.05.
946
947 **Figure 5: Effect of early life sugar or targeted *Parabacteroides* enrichment**
948 **on hippocampal gene expression.** (A) Pathway analyses for differentially expressed
949 genes (DEGs) at a p-value < 0.01 in hippocampal tissue punches from rats fed early life
950 sugar compared with controls. Upregulation by sugar is shown in red and

951 downregulation by sugar in blue. (B) A heatmap depicting DEGs that survived the
952 Benjamini-Hochberg corrected FDR of P< 0.05 in rats fed early life sugar compared
953 with controls. Warmer colors (red) signify an increase in gene expression and cool
954 colors (blue) a reduction in gene expression by treatment (CTL=control, SUG= early life
955 sugar; n=7/group). (C) A heatmap depicting DEGs that survived the Benjamini-
956 Hochberg corrected FDR of P< 0.05 in rats with early life *Parabacteroides* enrichment
957 compared with combined control groups. Warmer colors (red) signify an increase in
958 gene expression and cool colors (blue) a reduction in gene expression by treatment
959 (n=7, 14). (D) Pathway analyses for differentially expressed genes (DEGs) at a P-value <
960 0.01 in rats enriched with *Parabacteroides* compared with combined controls.
961 Upregulation by *Parabacteroides* transfer is shown in red and downregulation in blue.
962 Dotted line indicates ±0.25 log2 fold change.

Figure 1

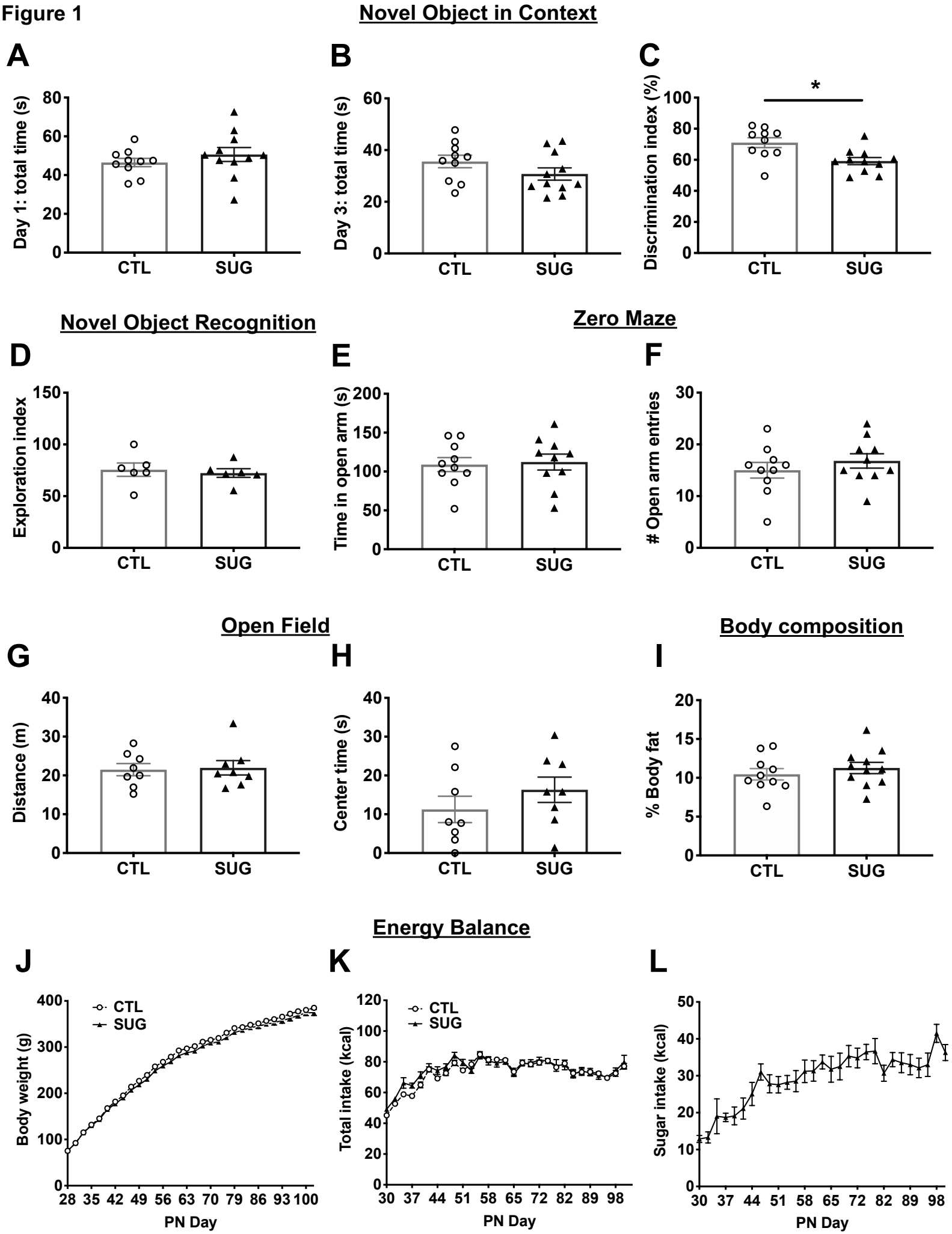
Novel Object in Context
A
Day 1: total time (s)
CTL
SUG
B
Day 3: total time (s)
C
Discrimination index (%)
*
Novel Object Recognition
D
Exploration index
Zero Maze
E
Time in open arm (s)
F
Open arm entries
Open Field
G
Distance (m)
H
Center time (s)
Body composition
I
% Body fat
Energy Balance
J
Body weight (g)
PN Day
K
Total intake (kcal)
L
Sugar intake (kcal)

Figure 2

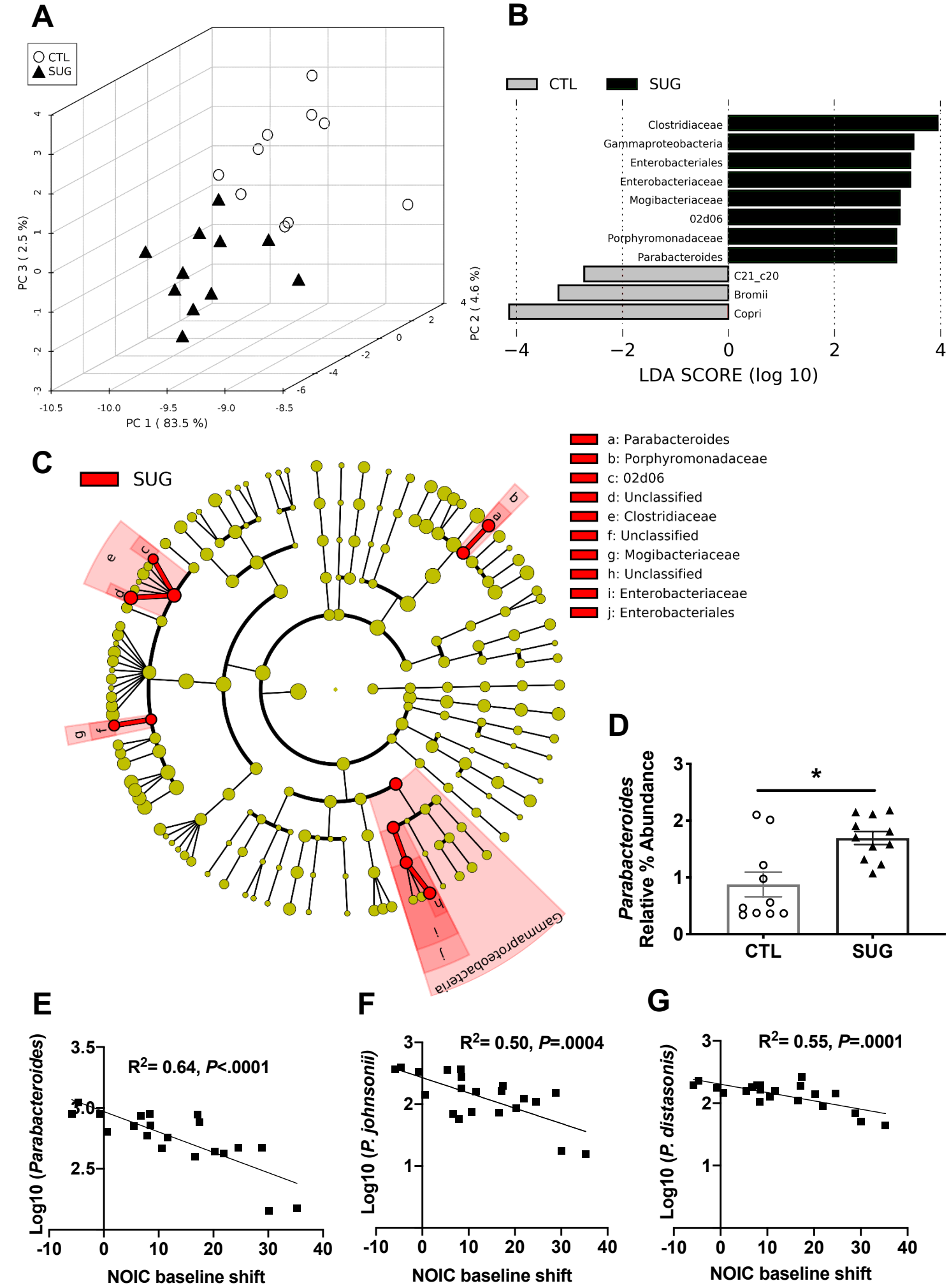
A
CTL
SUG
PC 3 (2.5 %)
PC 1 (83.5 %)
B
CTL
SUG
Clostridiaceae
Gammaproteobacteria
Enterobacteriales
Enterobacteriaceae
Mogibacteriaceae
02d06
Porphyromonadaceae
Parabacteroides
C21_c20
Bromii
Copri
PC 2 (4.6 %)
LDA SCORE (log 10)
C
SUG
a: Parabacteroides
b: Porphyromonadaceae
c: 02d06
d: Unclassified
e: Clostridiaceae
f: Unclassified
g: Mogibacteriaceae
h: Unclassified
i: Enterobacteriaceae
j: Enterobacteriales
Gammaproteobacteria
D
Parabacteroides Relative % Abundance
CTL
SUG
E
R2= 0.64, P<.0001
Log10 (Parabacteroides)
NOIC baseline shift
F
R2= 0.50, P=.0004
Log10 (P. johnsonii)
NOIC baseline shift
G
R2= 0.55, P=.0001
Log10 (P. distasonis)
NOIC baseline shift

Figure 3

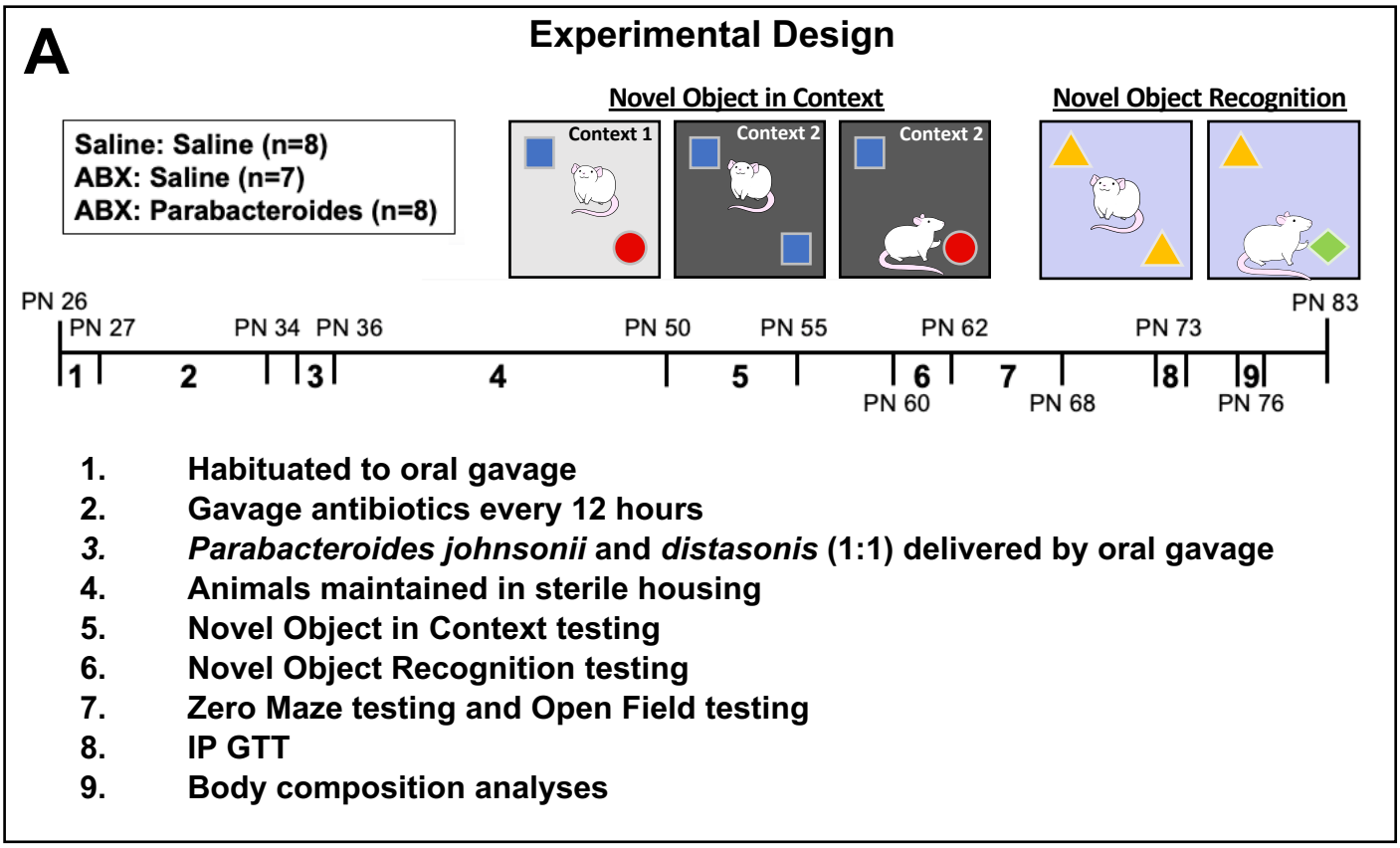
A
Experimental Design
Saline: Saline (n=8)
ABX: Saline (n=7)
ABX: Parabacteroides (n=8)
Novel Object in Context
Context 1
Context 2
Context 2
Novel Object Recognition
PN 26
PN 27
PN 34
PN 36
PN 50
PN 55
PN 62
PN 73
PN 83
PN 60
PN 68
PN 76
1
2
3
4
5
6
7
8
9
1. Habituated to oral gavage
2. Gavage antibiotics every 12 hours
3. Parabacteroides johnsonii and distasonis (1:1) delivered by oral gavage
4. Animals maintained in sterile housing
5. Novel Object in Context testing
6. Novel Object Recognition testing
7. Zero Maze testing and Open Field testing
8. IP GTT
9. Body composition analyses

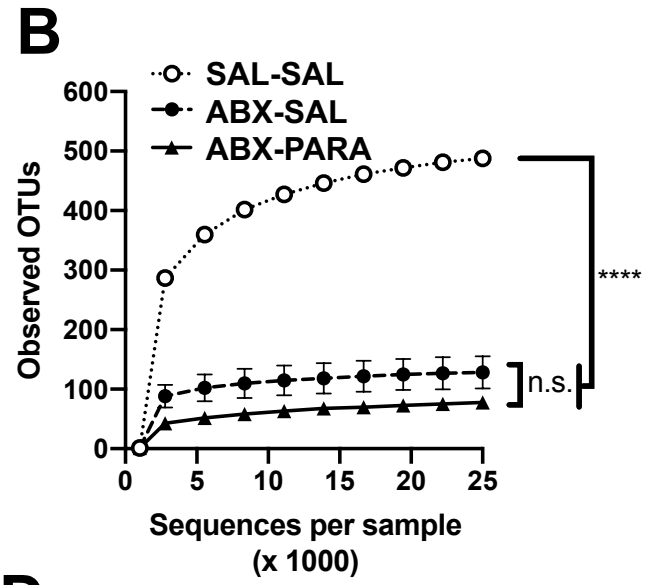
B
SAL-SAL
ABX-SAL
ABX-PARA
Observed OTUs
600
500
400
300
200
100
0
0
5
10
15
20
25
Sequences per sample
(x 1000)
****
n.s.

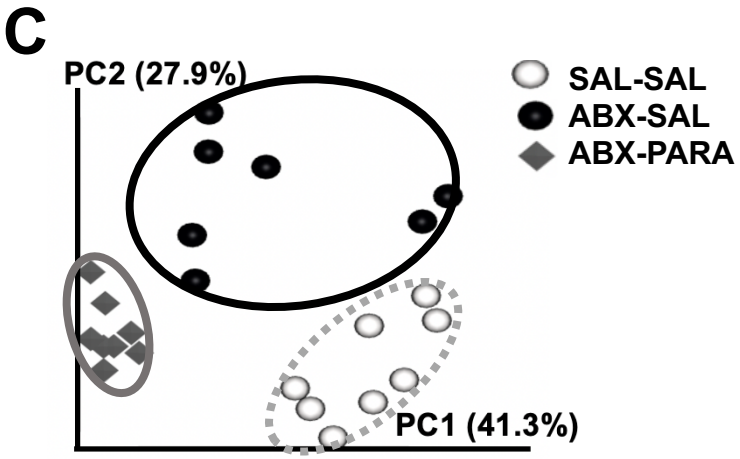
C
PC2 (27.9%)
PC1 (41.3%)
SAL-SAL
ABX-SAL
ABX-PARA

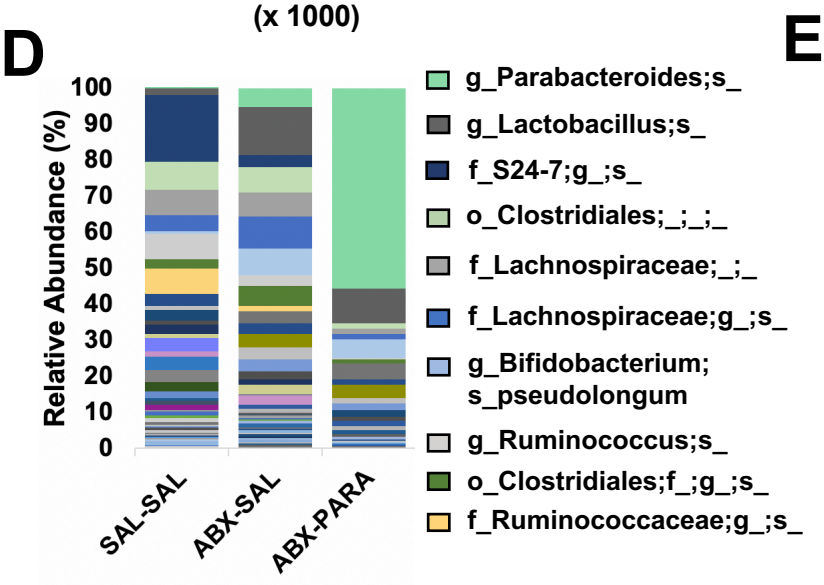
D
Relative Abundance (%)
100
90
80
70
60
50
40
30
20
10
0
SAL-SAL
ABX-SAL
ABX-PARA
g_Parabacteroides;s_
g_Lactobacillus;s_
f_S24-7;g_;s_
o_Clostridiales;_;_;_
f_Lachnospiraceae;_;_
f_Lachnospiraceae;g_;s_
g_Bifidobacterium;
s_pseudolongum
g_Ruminococcus;s_
o_Clostridiales;f_;g_;s_
f_Ruminococcaceae;g_;s_

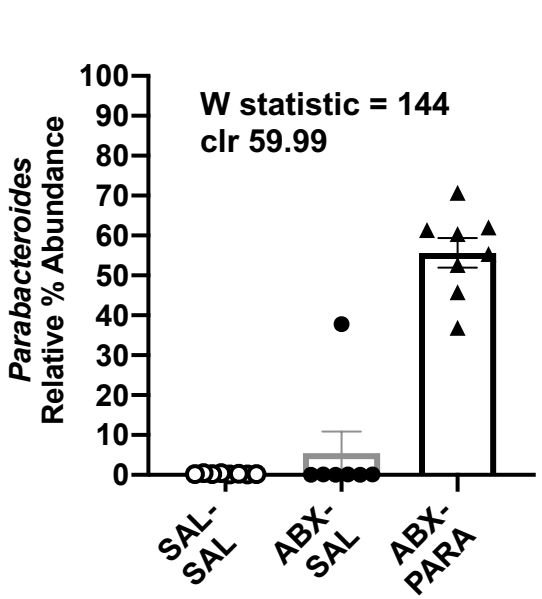
E
Parabacteroides
Relative % Abundance
W statistic = 144
clr 59.99
100
90
80
70
60
50
40
30
20
10
0
SAL-SAL
ABX-SAL
ABX-PARA

Figure 4

Novel Object in Context

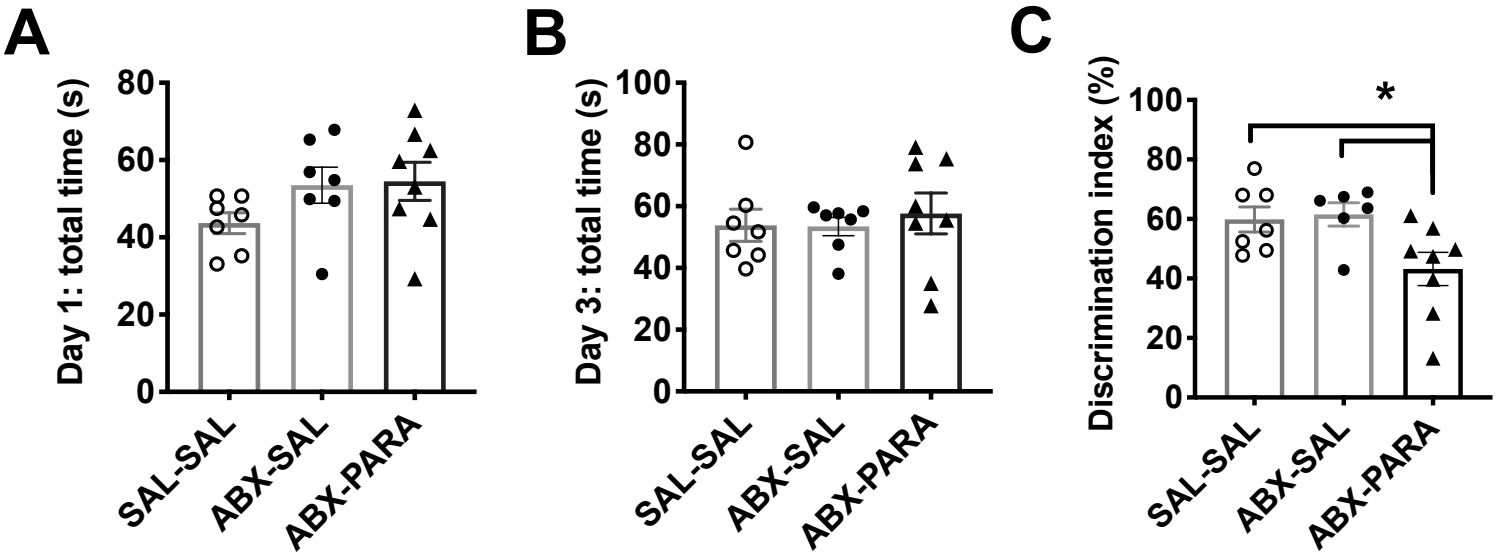

Novel Object Recognition

Zero Maze

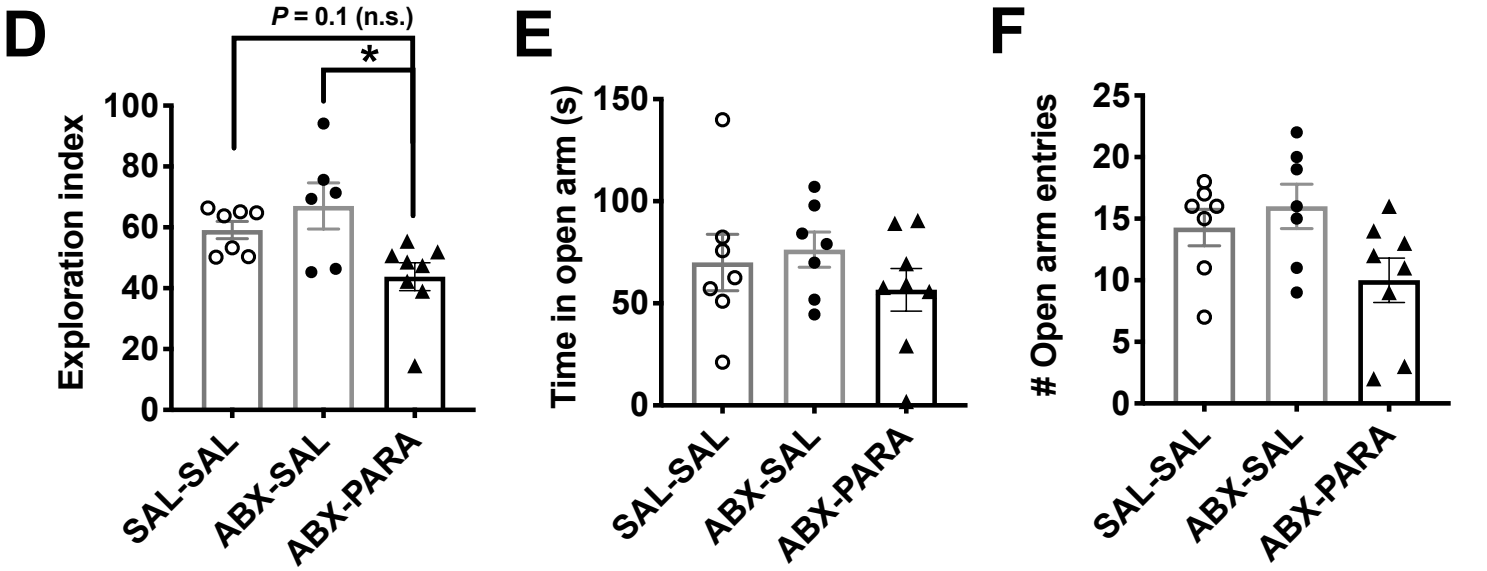

Open Field

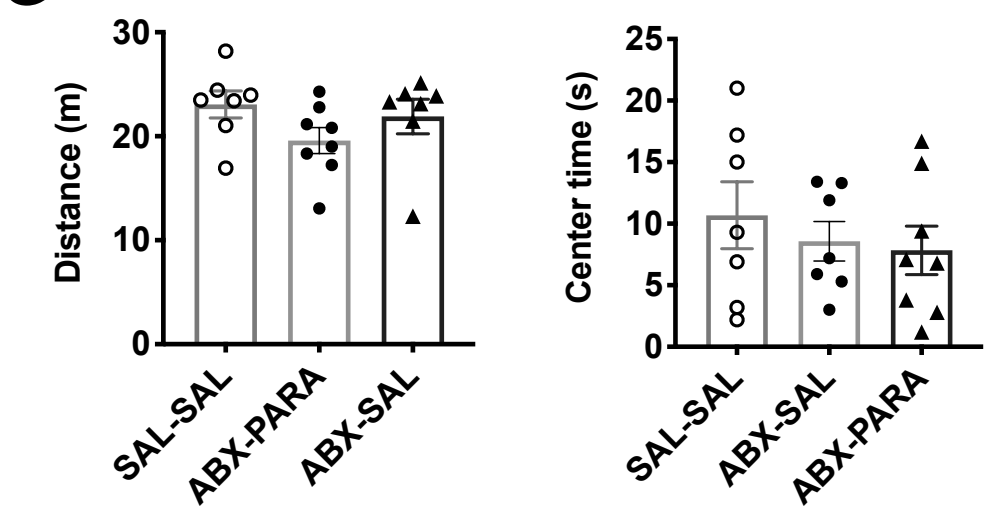

Table 1

Term	Overlap	P.value	Adjusted.P.value	Odds.Ratio	Combined.Score
cAMP signaling pathway	18/211	9.08710002926925e-07	0.000275339130886858	3.922209511	54.56279715
Long-term potentiation	10/67	1.75113958513324e-06	0.000265297647147685	6.862240522	90.96067106
Vascular smooth muscle contraction	14/140	2.31824837751272e-06	0.000234143086128785	4.597701149	59.65378698
Oxytocin signaling pathway	14/154	7.11610557675168e-06	0.000539044997438939	4.179728318	49.54294651
Circadian entrainment	11/99	1.02664310479357e-05	0.000622145721504906	5.108556833	58.68010783
Amphetamine addiction	9/68	1.58699502114579e-05	0.000801432485678624	6.085192698	67.24797055
Calcium signaling pathway	15/189	1.74937542122293e-05	0.000757229646615067	3.648969166	39.96959184
Cholinergic synapse	11/113	3.60773936379843e-05	0.00136643128403866	4.475638287	45.78508194
Axon guidance	14/180	4.14870567165781e-05	0.00139673090945813	3.575989783	36.08219845
Apelin signaling pathway	12/138	4.9577399145753e-05	0.00150219519411632	3.998001	39.62808792
Neurotrophin signaling pathway	11/121	6.78430713999647e-05	0.00186876823947175	4.179728318	40.11834187
Dopaminergic synapse	11/135	0.000181335935857366	0.00457873238039848	3.746275011	32.2747558
Glutamatergic synapse	10/114	0.000194050732212181	0.00452287475848392	4.033071184	34.47223604
Aldosterone synthesis and secretion	9/102	0.0003852671882922	0.00833828271803832	4.056795132	31.89279298
cGMP-PKG signaling pathway	12/172	0.000397324053301256	0.00802594587668537	3.207698476	25.11871164
Inflammatory mediator regulation of TRP channels	10/127	0.000464586599843255	0.00879810873453165	3.620237126	27.78301233
MAPK signaling pathway	16/294	0.000759189930175949	0.0135314440496066	2.502150285	17.97359249
GnRH signaling pathway	8/90	0.000767481845084928	0.0129192777255963	4.086845466	29.31247298
Glioma	7/75	0.0012196493427778	0.0194501974137724	4.291187739	28.79040196
Renin secretion	7/76	0.00131872717084366	0.0199787166382814	4.234724743	28.08083358
Retrograde endocannabinoid signaling	10/150	0.00167349865616307	0.0241461948960672	3.0651341	19.59490832
Neuroactive ligand-receptor interaction	17/348	0.00171069778931894	0.0235609740983472	2.246003435	14.30895981
Serotonergic synapse	9/132	0.00241588944480672	0.0318267174685407	3.134796238	18.88930332
Fc gamma R-mediated phagocytosis	7/87	0.00287625632706458	0.0363127361291903	3.699299775	21.64558595
Regulation of actin cytoskeleton	12/217	0.00294032709499641	0.0356367643913564	2.542507548	14.82087258
Dilated cardiomyopathy (DCM)	7/90	0.00347972133870684	0.0405521371395451	3.575989783	20.24297392
Apoptosis	9/141	0.00375836444668354	0.0421772010127819	2.934702861	16.38670992
Cocaine addiction	5/48	0.00377562901206963	0.040857699666325	4.789272031	26.7202504
Morphine addiction	7/92	0.00393256649864465	0.0410885396237699	3.498250875	19.37493308
Arrhythmogenic right ventricular cardiomyopathy (ARVC)	6/72	0.00476843186679707	0.0481611618546504	3.831417625	20.48175394
Proteoglycans in cancer	11/203	0.00502723467090038	0.0491371646865424	2.491365155	13.18650979
Ras signaling pathway	12/233	0.00518599384881057	0.0491048792559251	2.367914755	12.45947913
response to calcium ion (GO:0051592)	11/80	1.2352727119088e-06	0.00630359664887059	6.32183908	86.00368202
axon guidance (GO:0007411)	15/159	2.11788224048725e-06	0.00540377653660322	4.337453915	56.66924273
nervous system development (GO:0007399)	25/456	2.46003232910435e-05	0.0418451499180649	2.52066949	26.75123758
semaphorin-plexin signaling pathway (GO:0071526)	6/30	3.8991177233796e-05	0.0497429943560153	9.195402299	93.35333482
regulation of cAMP biosynthetic process (GO:0030817)	5/19	4.29910702140572e-05	0.0438766862604667	12.09921355	121.651762
integral component of plasma membrane (GO:0005887)	61/1464	7.0402625056926e-07	0.00031399570775389	1.915708812	27.13879347
dendrite (GO:0030425)	16/216	2.18212117029006e-05	0.00486613020974683	3.405704555	36.55216023
Hypothetical Network for Drug Addiction WP1246	6/31	4.74677094198248e-05	0.00835431685788917	8.898776418	88.59142051

Table 2

	Term	Overlap	P.value	Adjusted.P.va	Old.P.value	Old.Adjusted	Odds.Ratio	Combined.Sc	Genes	database
1	Ribosome	16/170	2.2535714016	0.0006828321	0	0	4.06555711	52.8644159	RPS7;RPS5;F	KEGG_2019_Mouse
2	Alzheimer disease	14/175	5.9653102426	0.0090374450	0	0	3.45572354	33.6136999	NDUFA13;ND	KEGG_2019_Mouse
3	Parkinson disease	12/144	0.0001349676	0.0136317326	0	0	3.59971202	32.0751456	NDUFA13;ND	KEGG_2019_Mouse
4	Valine, leucine and isoleucine degradation	7/56	0.0002964533	0.0224563378	0	0	5.39956803	43.8640434	BCKDHA;ALD	KEGG_2019_Mouse
5	Cardiac muscle contraction	8/78	0.0004410118	0.0267253189	0	0	4.4304148	34.2313287	UQCRQ;COX	KEGG_2019_Mouse
6	Hepatocellular carcinoma	12/171	0.0006547942	0.0330671074	0	0	3.03133644	22.2233021	TCF7L2;SMA	KEGG_2019_Mouse
7	cGMP-PKG signaling pathway	12/172	0.0006895098	0.0298459255	0	0	3.01371239	21.9384086	ATF2;PPP1R	KEGG_2019_Mouse
8	Colorectal cancer	8/88	0.0009893071	0.0374700074	0	0	3.92695857	27.1686854	TCF7L2;SMA	KEGG_2019_Mouse
9	Fatty acid degradation	6/50	0.0009995403	0.0336511912	0	0	5.18358531	35.8093221	ACADL;ECI1;	KEGG_2019_Mouse
10	Thermogenesis	14/231	0.0010310146	0.0312397432	0	0	2.61797238	18.0043508	ATF2;NDUFA	KEGG_2019_Mouse
11	Oxidative phosphorylation	10/134	0.0011365669	0.0313072522	0	0	3.22362271	21.8553336	NDUFA13;ND	KEGG_2019_Mouse
12	Dopaminergic synapse	10/135	0.0012027348	0.0303690537	0	0	3.19974402	21.5123824	ATF2;GRIA2;I	KEGG_2019_Mouse
13	Vascular smooth muscle contraction	10/140	0.0015824106	0.0368823395	0	0	3.08546745	19.8975807	PPP1R12A;AI	KEGG_2019_Mouse
14	Endocrine and other factor-regulated calcium reabsorption	6/55	0.0016548484	0.0358156477	0	0	4.71235028	30.1781074	GNAQ;BDKRI	KEGG_2019_Mouse
15	Pathways in cancer	24/535	0.0016621713	0.0335758610	0	0	1.9377889	12.401133	RET;TCF7L2;	KEGG_2019_Mouse
16	Huntington disease	12/192	0.0017815419	0.0337379513	0	0	2.69978402	17.090378	NDUFA13;ND	KEGG_2019_Mouse
17	Endometrial cancer	6/58	0.0021800554	0.0388562817	0	0	4.46860803	27.3854397	TCF7L2;APC;	KEGG_2019_Mouse
18	Gastric cancer	10/150	0.0026327375	0.0443177484	0	0	2.87976962	17.1050571	TCF7L2;SMA	KEGG_2019_Mouse
19	Non-alcoholic fatty liver disease (NAFLD)	10/151	0.0027627966	0.0440593356	0	0	2.8606983	16.8538379	NDUFA13;ND	KEGG_2019_Mouse
20	SRP-dependent cotranslational protein targeting to membrane (GO:0	16/90	2.3456175755	1.1969686487	0	0	7.67938565	170.277339	RPS7;RPS5;F	GO_Biological_Process_2018
21	protein targeting to ER (GO:0045047)	16/98	8.7398242692	2.2299661623	0	0	7.05249702	147.100707	RPS7;RPS5;F	GO_Biological_Process_2018
22	viral transcription (GO:0019083)	17/114	1.1115537635	1.8907529518	0	0	6.44158994	132.809526	RANBP2;RPS	GO_Biological_Process_2018
23	cotranslational protein targeting to membrane (GO:0006613)	15/94	4.0895658105	5.2172635828	0	0	6.89306558	133.138369	RPS7;RPS5;F	GO_Biological_Process_2018
24	viral gene expression (GO:0019080)	16/111	5.7091825356	5.8267916958	0	0	6.2265289	118.186928	RANBP2;RPS	GO_Biological_Process_2018
25	nuclear-transcribed mRNA catabolic process, nonsense-mediated de	15/113	5.3284114672	4.5318139528	0	0	5.73405455	96.0318102	RPS7;RPS5;F	GO_Biological_Process_2018
26	cellular protein metabolic process (GO:0044267)	31/485	3.8477509014	0.0002805010	0	0	2.76101623	40.7818853	RPLP0;RPL1	GO_Biological_Process_2018
27	cytoplasmic translation (GO:0002181)	10/55	4.6181807744	0.0002945822	0	0	7.85391714	114.573688	RPS7;RPLP0	GO_Biological_Process_2018
28	nuclear-transcribed mRNA catabolic process (GO:0000956)	17/175	6.9899324550	0.0003963291	0	0	4.19623573	59.4758706	RPS7;RPS5;F	GO_Biological_Process_2018
29	peptide biosynthetic process (GO:0043043)	17/175	6.9899324550	0.0003566962	0	0	4.19623573	59.4758706	RPS7;MRPS2	GO_Biological_Process_2018
30	rRNA metabolic process (GO:0016072)	18/201	1.0939569396	0.0005074965	0	0	3.86834725	53.0958095	UTP15;RPS7;	GO_Biological_Process_2018
31	rRNA processing (GO:0006364)	18/203	1.2630718406	0.0005371213	0	0	3.83023545	52.0221194	UTP15;RPS7;	GO_Biological_Process_2018
32	translation (GO:0006412)	19/233	2.2650960072	0.0008891373	0	0	3.52246498	45.7846244	MRPS24;RPS	GO_Biological_Process_2018
33	viral process (GO:0016032)	18/221	4.2461156389	0.0015477091	0	0	3.51827057	43.5192688	RANBP2;RPS	GO_Biological_Process_2018
34	mitochondrial ATP synthesis coupled electron transport (GO:004277	11/86	4.6602675569	0.0015854230	0	0	5.52513938	67.8290294	NDUFA13;ND	GO_Biological_Process_2018
35	ribosome biogenesis (GO:0042254)	18/227	6.1737508478	0.0019690406	0	0	3.42527664	41.086892	UTP15;RPS7;	GO_Biological_Process_2018
36	ncRNA processing (GO:0034470)	18/228	6.5623672682	0.0019698682	0	0	3.4102535	40.698508	UTP15;RPS7;	GO_Biological_Process_2018
37	respiratory electron transport chain (GO:0022904)	11/95	1.2341294187	0.0034987569	0	0	5.00170513	56.5320706	NDUFA13;ND	GO_Biological_Process_2018
38	gene expression (GO:0010467)	24/412	3.6661542004	0.0098465183	0	0	2.51630355	25.7009765	RANBP2;RPS	GO_Biological_Process_2018
39	fatty acid oxidation (GO:0019395)	7/51	0.0001634500	0.0417042818	0	0	5.92893745	51.6944239	ACADL;ECI1;	GO_Biological_Process_2018
40	fatty acid beta-oxidation (GO:0006635)	7/51	0.0001634500	0.0397183636	0	0	5.92893745	51.6944239	ACADL;ECI1;	GO_Biological_Process_2018
41	ribosome (GO:0005840)	14/77	2.3166517915	1.0332266990	0	0	7.85391714	156.160557	RPS7;DHX9;F	GO_Cellular_Component_2018
42	cytosolic ribosome (GO:0022626)	16/125	3.2420827636	7.2298445629	0	0	5.52915767	95.3473647	RPS7;RPS5;F	GO_Cellular_Component_2018
43	polysomal ribosome (GO:0042788)	8/29	2.1739502116	3.2319393146	0	0	11.9162881	182.814327	RPL7A;DHX9	GO_Cellular_Component_2018
44	cytosolic part (GO:0044445)	16/160	1.0068540108	0.0001122642	0	0	4.31965443	59.6487254	RPS7;RPS5;F	GO_Cellular_Component_2018
45	polysome (GO:0005844)	10/64	1.9857457595	0.0001771285	0	0	6.74946004	88.6171437	RPL7A;DHX9	GO_Cellular_Component_2018
46	cytosolic small ribosomal subunit (GO:0022627)	8/50	1.7758618489	0.0013200573	0	0	6.91144708	75.6018288	RPS27;RPS7	GO_Cellular_Component_2018
47	small ribosomal subunit (GO:0015935)	8/54	3.1741224241	0.0020223694	0	0	6.39948804	66.2852205	RPS27;RPS7	GO_Cellular_Component_2018
48	cytosolic large ribosomal subunit (GO:0022625)	8/70	0.0002085490	0.0116266070	0	0	4.93674792	41.8405998	RPL7A;RPLP	GO_Cellular_Component_2018
49	large ribosomal subunit (GO:0015934)	8/73	0.0002795591	0.0138537081	0	0	4.73386787	38.7339115	RPL7A;RPLP	GO_Cellular_Component_2018
50	ficolin-1-rich granule lumen (GO:1904813)	10/124	0.0006237135	0.0278176225	0	0	3.48359228	25.7082819	EEF1A1;ALAI	GO_Cellular_Component_2018
51	endocytic vesicle lumen (GO:0071682)	4/18	0.0006702942	0.0271773869	0	0	9.59923206	70.1492075	SPARC;HBB;/	GO_Cellular_Component_2018
52	mitochondrial inner membrane (GO:0005743)	18/342	0.0011028826	0.0409904699	0	0	2.27350233	15.4821598	NDUFA13;ND	GO_Cellular_Component_2018
53	RNA binding (GO:0003723)	56/1388	3.4592110509	0.0398155191	0	0	1.74280006	17.9018416	OTUD4;CELF	GO_Molecular_Function_2018
54	RNA polymerase binding (GO:0070063)	5/19	5.7845249375	0.0332899410	0	0	11.3675117	110.921214	ZFP36;DHX9;	GO_Molecular_Function_2018
55	Cytoplasmic Ribosomal Proteins WP163	15/92	3.0072409788	5.2927441227	0	0	7.04291483	138.197785	RPS7;RPS5;F	WikiPathways_2019_Mouse
56	Fatty Acid Beta Oxidation WP1269	7/34	1.0660091045	0.0009380880	0	0	8.89340617	101.820639	ACADL;GK;E	WikiPathways_2019_Mouse
57	Mitochondrial LC-Fatty Acid Beta-Oxidation WP401	5/16	2.3013966424	0.0013501526	0	0	13.4989201	144.160493	ACADL;ECI1;	WikiPathways_2019_Mouse
58	mRNA processing WP310	22/457	0.0010577431	0.0465406987	0	0	2.07948353	14.2478263	RNASEH2A;F	WikiPathways_2019_Mouse
59	Fatty acid oxidation WP2318	3/10	0.0013102260	0.0461199575	0	0	12.9589633	86.0158391	ACADM;HADI	WikiPathways_2019_Mouse

Supplemental Figure Legends:

Figure S1: Effect of early life sugar consumption on food intake and metabolic measures (A, B) There were no differences in lean mass or in fat mass between animals fed sugar solutions or control animals (n=10,11; two-tailed, type 2 Student's T-test). (C) Kcals from chow intake were lower throughout the feeding period in animals fed early life sugar (n=10,11). (D) Results from the intraperitoneal glucose tolerance test show an elevated area under the curve (AUC) in rodents fed sugar solutions during early life (n=10,11; two-tailed, type 2 Student's T-test; P<.05). CTL=control, SUG= sugar, PN= post-natal day; data shown as mean ± SEM.

Figure S2: Relationship between *Parabacteroides* and behavioral outcomes in the Novel Object in Context task (NOIC) A) Linear regression of log normalized fecal *Parabacteroides* counts against shift from baseline performance scores in the NOIC task in sugar (SUG) and control (CTL) groups (n=10, 11). (B, C) Linear regression of the most abundant fecal *Parabacteroides* species against shift from baseline performance scores in NOIC across all groups tested (n=10, 11). *P<0.05; data shown as mean ± SEM.

Figure S3: Effect of early life sugar consumption on the rat cecal microbiota (A) Principal component analysis (PCA) was run using all phylogenic levels (112 normalized taxa abundances) and shows different clustering patterns based on overall cecal microbial profiles. (B) Linear discriminant analysis (LDA) Effect Size (LEfSe), run using the GALAXY platform, identified characteristic features of the cecal microbiota of

rats fed a control diet or early life sugar. Relative differences among groups were used to rank the features with the LDA score set at 2. (C) Identified taxa are displayed by scores and on a phylogenic cladogram. CTL=control, SUG= sugar.

Figure S4: Effect of early life sugar consumption on the rat fecal microbiota. Filtered bacterial abundances by taxonomic levels phylum, class, order, family, genus in fecal samples from rats fed a control diets or early life sugar. Differences in abundances were assessed by Mann-Whitney non-parametric test. * $p<0.05$, *** $p<0.001$. CTL=control, SUG= sugar.

Figure S5: Effect of early life sugar consumption on the rat cecal microbiota: Filtered bacterial abundances by taxonomic levels phylum, class, order, family, genus in cecal samples from rats fed a control diets or early life sugar. Differences in abundances were assessed by Mann-Whitney non-parametric test. * $p<0.05$, *** $p<0.001$. CTL=control, SUG= sugar.

57 **Phylogenic taxonomy legend for Figure S4, S5:**

58

Phylum		Class		Order		Family		Genus
F	*Firmicutes*	C	*Clostridia*	C	*Clostridiales*	C	*Clostridiaceae*	*Clostridium*
						L	*Lachnospiraceae*	*Coprococcus*
								Blautia
								Dorea
						P	*Peptococcaceae*	
						Ps	*Peptostreptococcaceae*	
						R	*Ruminococcaceae*	*Oscillospira*
								Ruminococcus
		B	*Bacilli*	L	*Lactobacillales*	L	*Lactobacillaceae*	*Lactobacillus*
				T	*Turicibacterales*	T	*Turicibacteraceae*	*Turicibacter*
				B	*Bacillales*			
		E	*Erysipelotrichi*	E	*Erysipelotrichales*	E	*Erysipelotrichaceae*	*Allobaculum*
B	*Bacteroidetes*	B	*Bacteroidia*	B	*Bacteroidales*	S	*S24-7*	
						B	*Bacteroidaceae*	*Bacteroides*
						P	*Prevotellaceae*	*Prevotella*
								Paraprevotella
						Po	*Porphyromonadaceae*	*Parabacteroides*
V	*Verrucomicrobia*	V	*Verrucomicrobiae*	V	*Verrucomicrobiales*	V	*Verrucomicrobiaceae*	*Akkermansia*
P	*Proteobacteria*	β	*Betaproteobacteria*	B	*Burkholderiales*	S	*Sutterellaceae*	*Sutterella*
		Δ	*Deltaproteobacteria*	D	*Desulfovibrionales*	D	*Desulfovibrionaceae*	*Desulfovibrio*
								Bilophila
T	*Tenericutes*	M	*Mollicutes*	RF	*RF39*			
D	*Deferribacteres*	D	*Deferribacteres*	D	*Deferribacterales*	D	*Deferribacteraceae*	*Mucispirillum*
A	*Actinobacteria*	A	*Actinobacteria*	B	*Bifidobacter*	B	*Bifidobacteriaceae*	

59
60
61

62 **Figure S6: Experimental design, food intake, and metabolic measures for**

63 **gut *Parabacteroides* enrichment** (A) Effect of antibiotic treatment on food intake

64 (B) and body weight (n=7,8). (C) Effect of gut *Parabacteroides* enrichment on body

65 weight at PN 51 prior to the start of behavioral testing (n=7,8; one way ANOVA with

66 Tukey's post hoc test, $F_{(2,20)}$= 8.79; *P<.05) (D) Effect of gut *Parabacteroides*

67 enrichment on body weight (n=7,8; one way ANOVA with Tukey's post hoc test, $F_{(2,19)}$=

68 5.7; *P<.05) (E) lean mass (n=7,8; one way ANOVA with Tukey's post hoc test, $F_{(2,19)}$=

69 5.33; *P<.05) (F) and body fat (one way ANOVA, n.s.) at PN 76. (G) Blood glucose levels

70 during an interaperitoneal glucose tolerance test (IP GTT) (n=7,8 one way ANOVA for

71 AUC; n.s.) SAL-SAL=saline-saline control, ABX-SAL= antibiotics-saline control, ABX-

72 PARA= antibiotics-*P. johnsonii* and *P. distasonis* enriched, PN= post-natal day; data
73 shown as mean ± SEM.
74
75 **Figure S7: Principal component analyses (PCA) of hippocampal gene**
76 **expression data to identify outliers** (A) PCA identified one control sample (red
77 arrow) as an outlier when all samples from both sugar and *Parabacteroides* enrichment
78 experiments were considered. (B) PCA identified one treatment sample (red arrow)
79 from the *Parabacteroides* experiment as an outlier. After removing the outliers, PCA
80 for the remaining samples from the sugar treatment experiment (C) and those from the
81 *Parabacteroides* enrichment experiments (D).
82
83 **Figure S8: Comparison of hippocampal gene expression pathways altered**
84 **by sugar and *Parabacteriodes*.** The dopaminergic synapse pathway overlaps in the
85 sugar and *Parabacteroides* transfer experiments. Red= upregulated by sugar, dark
86 blue= downregulated by sugar, orange= upregulated by *Parabacteroides*, light blue=
87 downregulated by *Parabacteroides*. * $P < 0.05$ and ** $P < 0.01$. Dotted line indicated ±
88 0.25 log2 fold change.

Figure S1

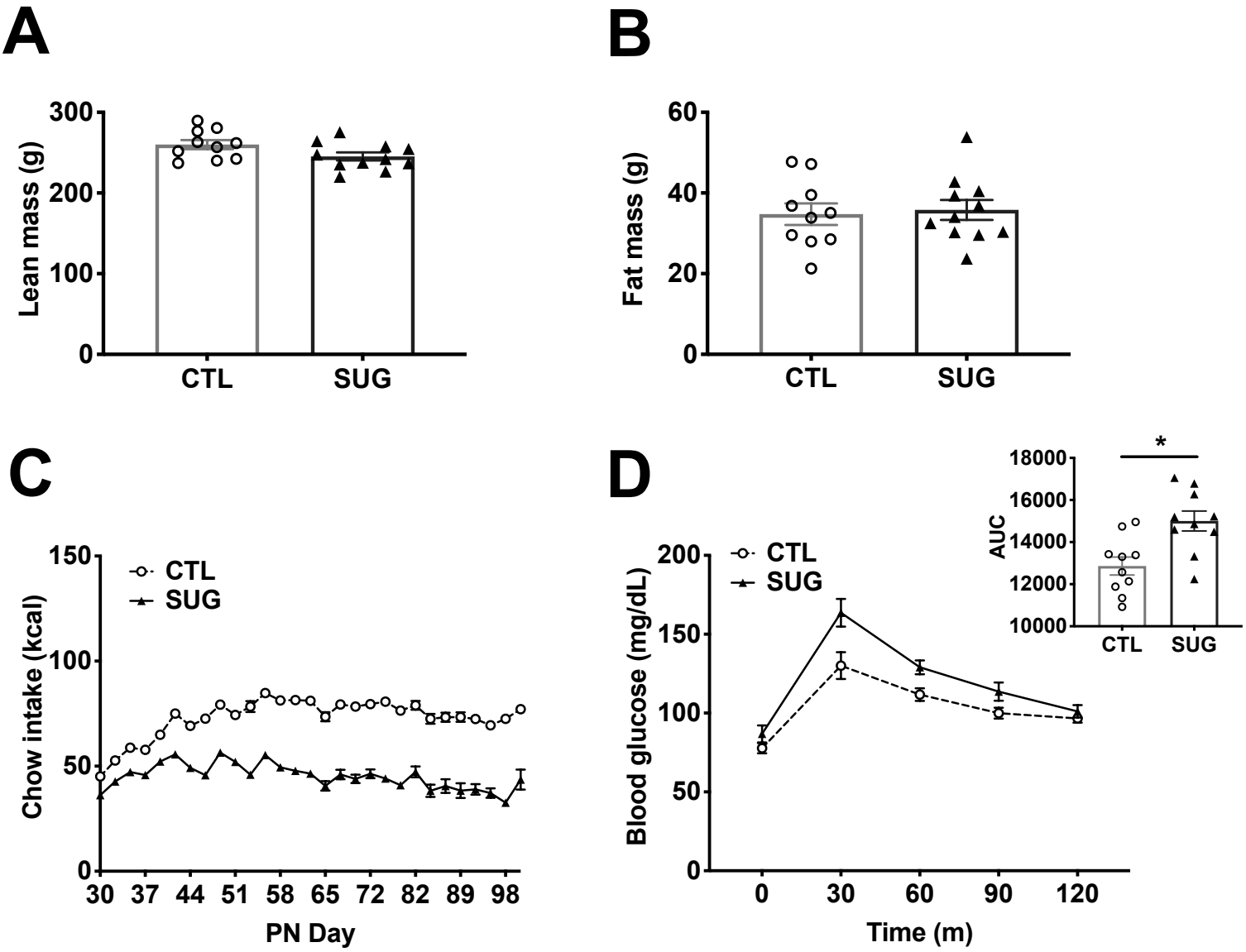
A
Lean mass (g)
300
200
100
0
CTL
SUG
B
Fat mass (g)
60
40
20
0
CTL
SUG
C
Chow intake (kcal)
150
100
50
0
CTL
SUG
30 37 44 51 58 65 72 82 89 98
PN Day
D
Blood glucose (mg/dL)
200
150
100
50
0
CTL
SUG
0 30 60 90 120
Time (m)
AUC
18000
16000
14000
12000
10000
*
CTL
SUG

Figure S2

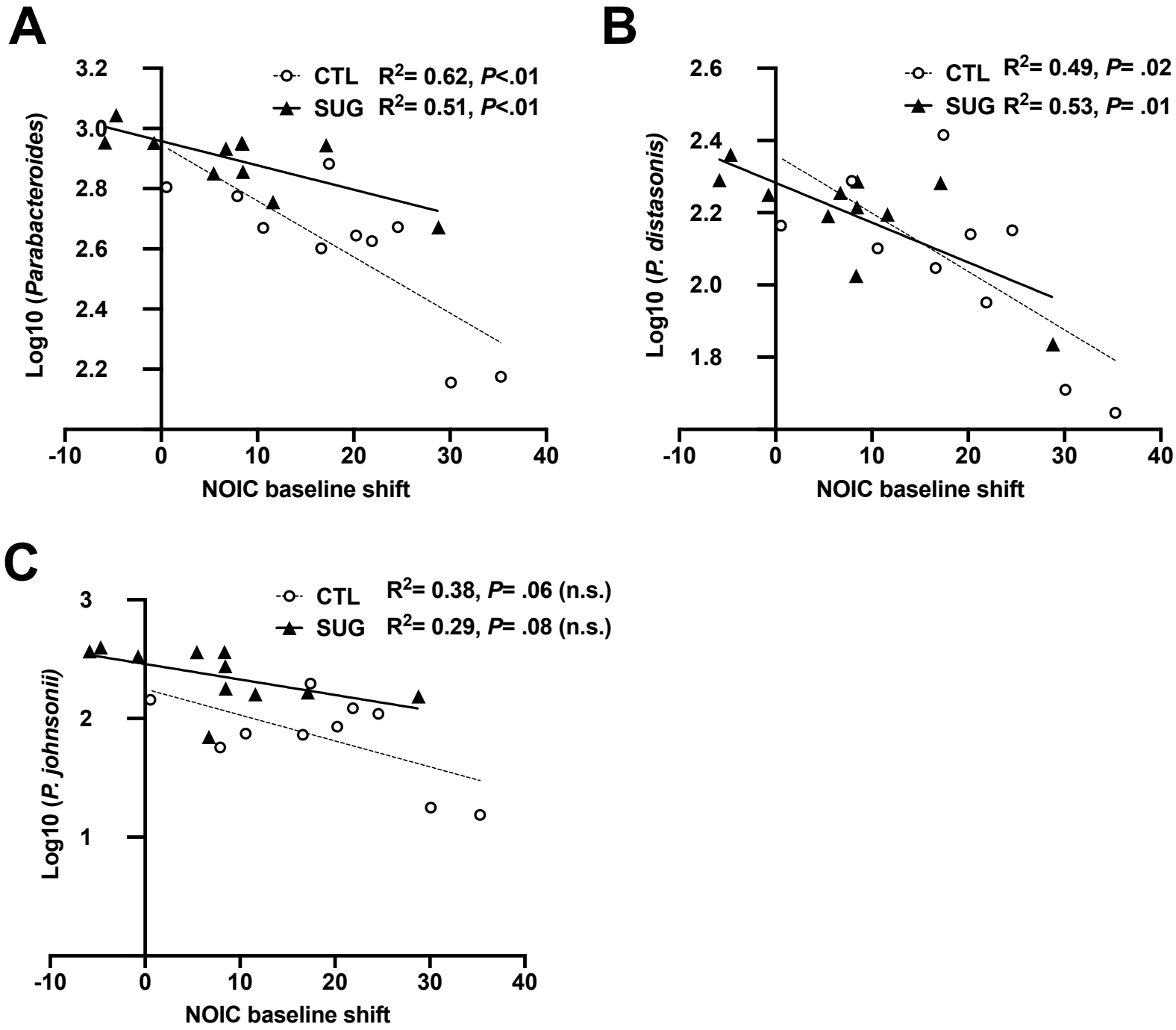
A
CTL R2= 0.62, P<.01
SUG R2= 0.51, P<.01
Log10 (Parabacteroides)
3.2
3.0
2.8
2.6
2.4
2.2
-10
0
10
20
30
40
NOIC baseline shift
B
CTL R2= 0.49, P= .02
SUG R2= 0.53, P= .01
Log10 (P. distasonis)
2.6
2.4
2.2
2.0
1.8
-10
0
10
20
30
40
NOIC baseline shift
C
CTL R2= 0.38, P= .06 (n.s.)
SUG R2= 0.29, P= .08 (n.s.)
Log10 (P. johnsonii)
3
2
1
-10
0
10
20
30
40
NOIC baseline shift

Figure S3

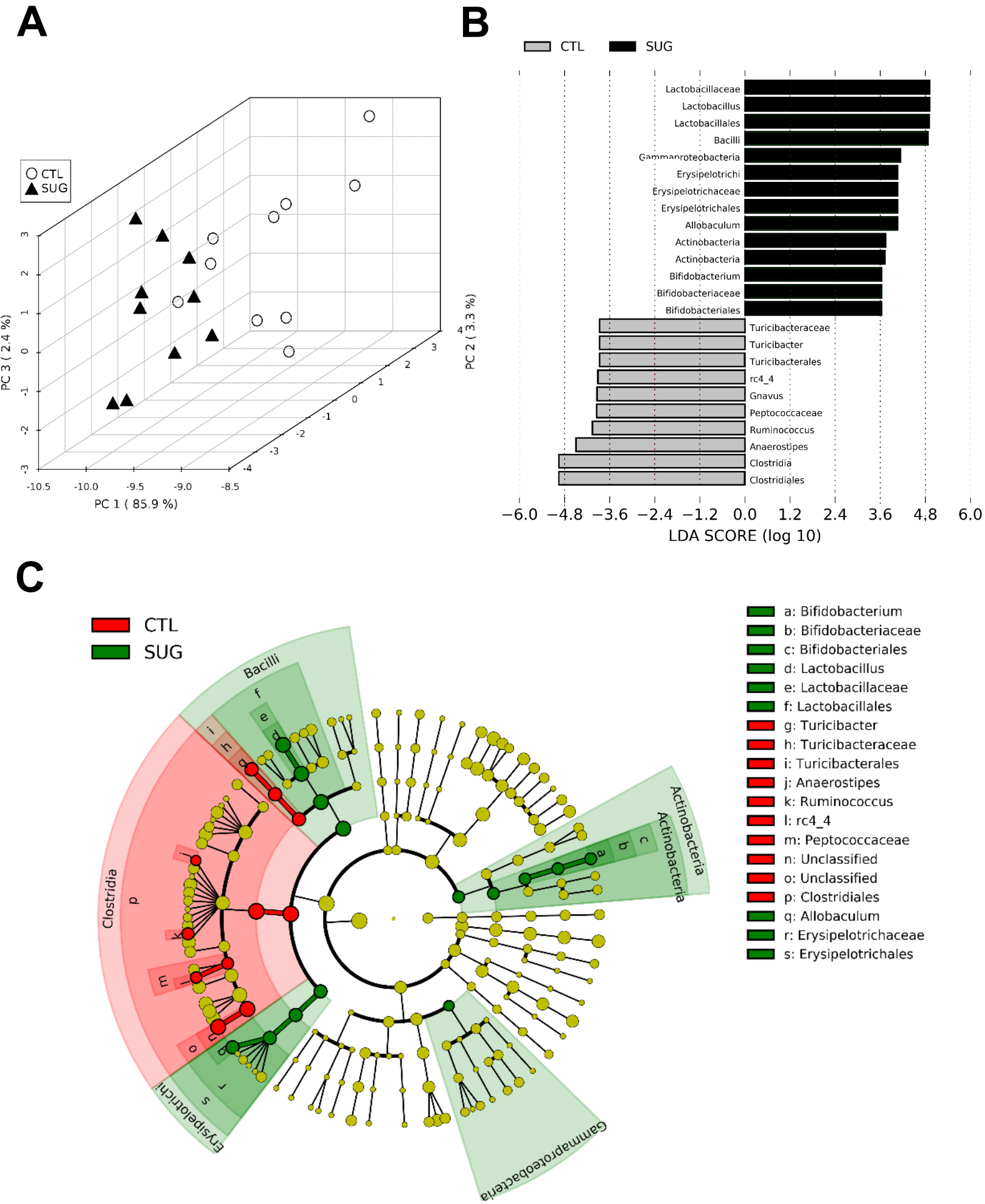
A
CTL
SUG
PC 1 (85.9 %)
PC 2 (3.3 %)
PC 3 (2.4 %)
B
CTL
SUG
Lactobacillaceae
Lactobacillus
Lactobacillales
Bacilli
Gammaproteobacteria
Erysipelotrichi
Erysipelotrichaceae
Erysipelotrichales
Allobaculum
Actinobacteria
Actinobacteria
Bifidobacterium
Bifidobacteriaceae
Bifidobacteriales
Turicibacteraceae
Turicibacter
Turicibacterales
rc4_4
Gnavus
Peptococcaceae
Ruminococcus
Anaerostipes
Clostridia
Clostridiales
LDA SCORE (log 10)
C
CTL
SUG
Bacilli
Clostridia
Erysipelotrichi
Actinobacteria
Actinobacteria
Gammaproteobacteria
a: Bifidobacterium
b: Bifidobacteriaceae
c: Bifidobacteriales
d: Lactobacillus
e: Lactobacillaceae
f: Lactobacillales
g: Turicibacter
h: Turicibacteraceae
i: Turicibacterales
j: Anaerostipes
k: Ruminococcus
l: rc4_4
m: Peptococcaceae
n: Unclassified
o: Unclassified
p: Clostridiales
q: Allobaculum
r: Erysipelotrichaceae
s: Erysipelotrichales

Figure S4

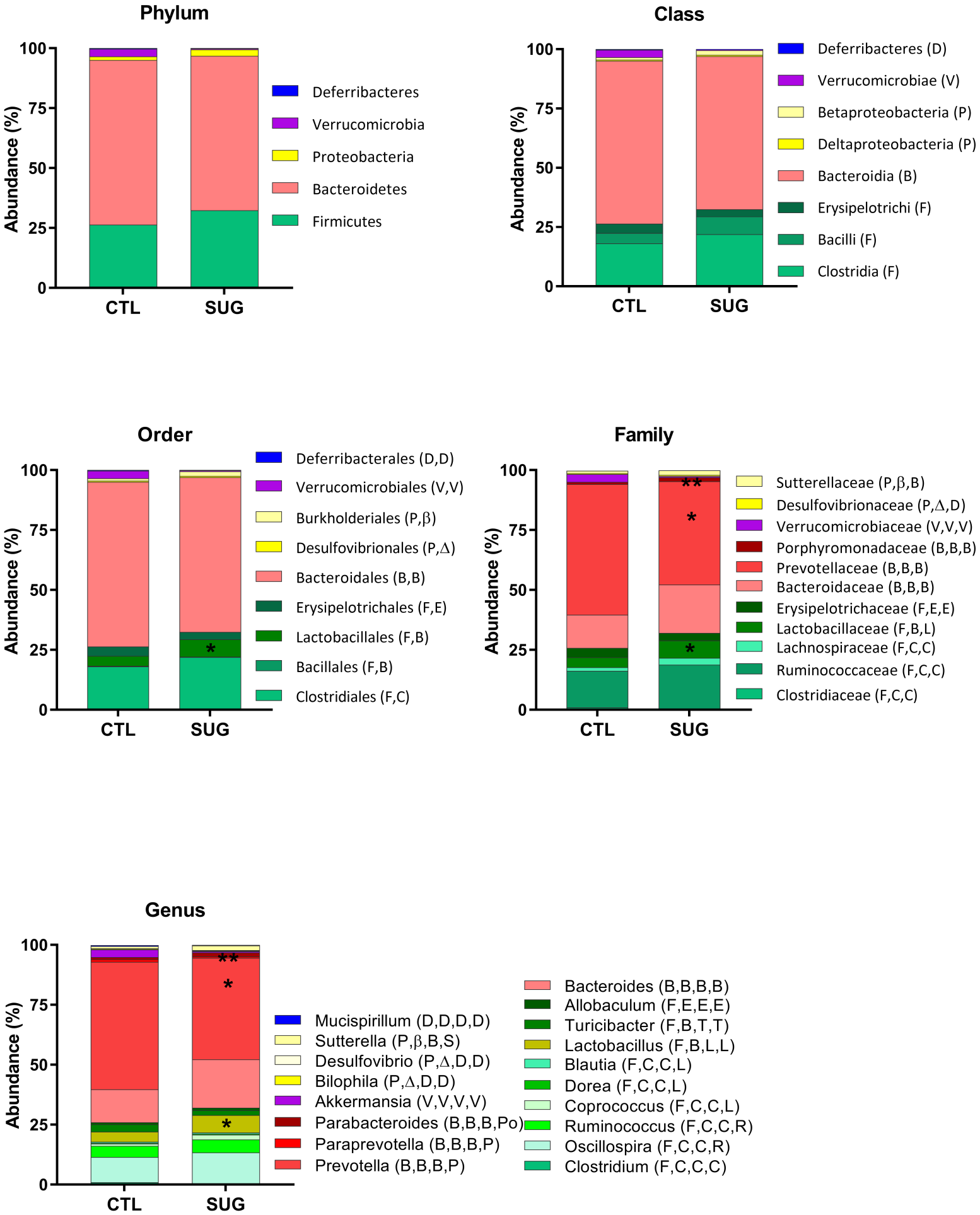
Phylum
Abundance (%)
100
75
50
25
0
CTL
SUG
Deferribacteres
Verrucomicrobia
Proteobacteria
Bacteroidetes
Firmicutes
Class
Deferribacteres (D)
Verrucomicrobiae (V)
Betaproteobacteria (P)
Deltaproteobacteria (P)
Bacteroidia (B)
Erysipelotrichi (F)
Bacilli (F)
Clostridia (F)
Order
Deferribacterales (D,D)
Verrucomicrobiales (V,V)
Burkholderiales (P,β)
Desulfovibrionales (P,Δ)
Bacteroidales (B,B)
Erysipelotrichales (F,E)
Lactobacillales (F,B)
Bacillales (F,B)
Clostridiales (F,C)
*
Family
Sutterellaceae (P,β,B)
Desulfovibrionaceae (P,Δ,D)
Verrucomicrobiaceae (V,V,V)
Porphyromonadaceae (B,B,B)
Prevotellaceae (B,B,B)
Bacteroidaceae (B,B,B)
Erysipelotrichaceae (F,E,E)
Lactobacillaceae (F,B,L)
Lachnospiraceae (F,C,C)
Ruminococcaceae (F,C,C)
Clostridiaceae (F,C,C)
**
*
Genus
Mucispirillum (D,D,D,D)
Sutterella (P,β,B,S)
Desulfovibrio (P,Δ,D,D)
Bilophila (P,Δ,D,D)
Akkermansia (V,V,V,V)
Parabacteroides (B,B,B,Po)
Paraprevotella (B,B,B,P)
Prevotella (B,B,B,P)
Bacteroides (B,B,B,B)
Allobaculum (F,E,E,E)
Turicibacter (F,B,T,T)
Lactobacillus (F,B,L,L)
Blautia (F,C,C,L)
Dorea (F,C,C,L)
Coprococcus (F,C,C,L)
Ruminococcus (F,C,C,R)
Oscillospira (F,C,C,R)
Clostridium (F,C,C,C)

Figure S5

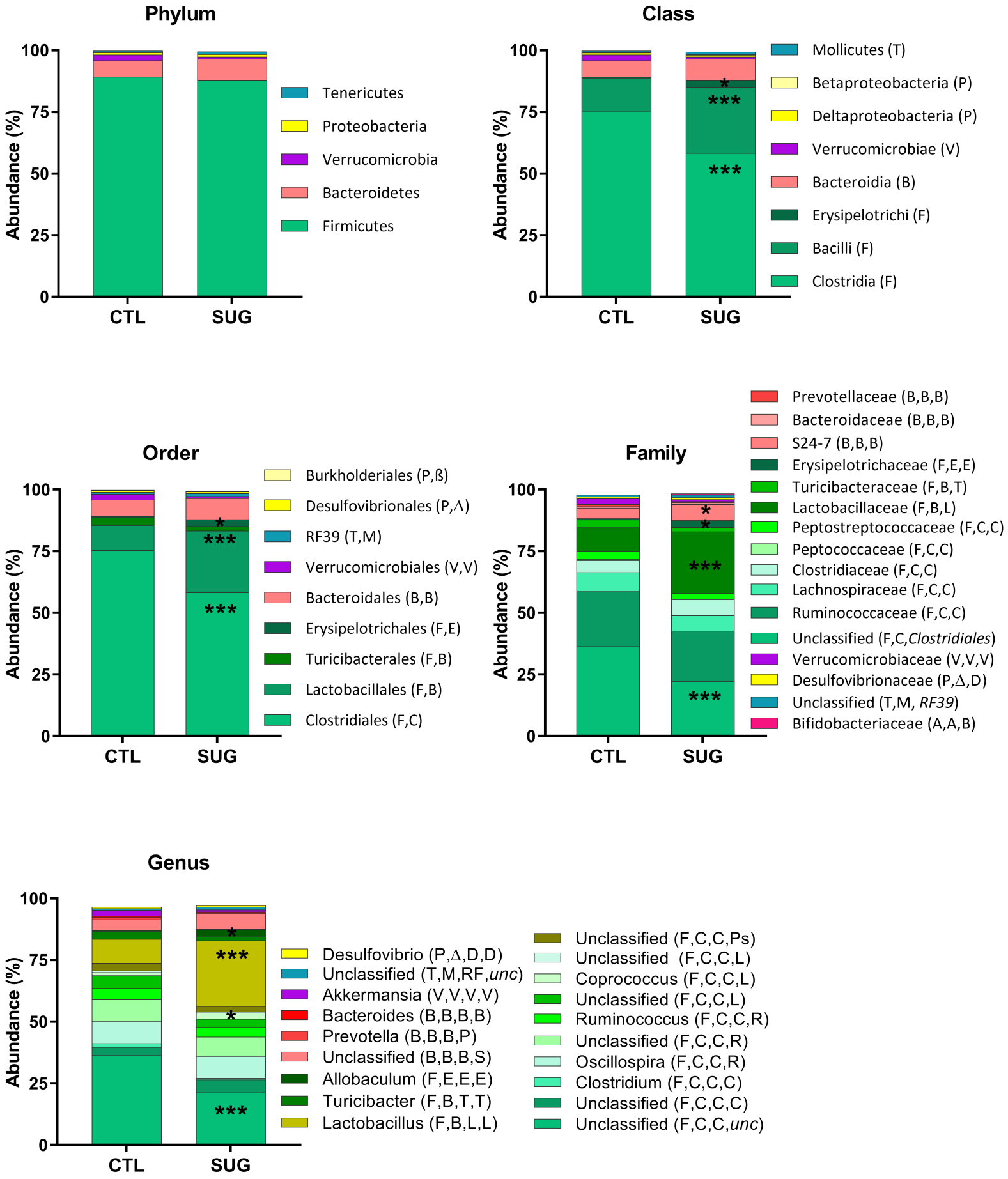
Phylum
Abundance (%)
100
75
50
25
0
CTL
SUG
Tenericutes
Proteobacteria
Verrucomicrobia
Bacteroidetes
Firmicutes
Class
Mollicutes (T)
Betaproteobacteria (P)
Deltaproteobacteria (P)
Verrucomicrobiae (V)
Bacteroidia (B)
Erysipelotrichi (F)
Bacilli (F)
Clostridia (F)
*
***
***
Order
Burkholderiales (P,ß)
Desulfovibrionales (P,Δ)
RF39 (T,M)
Verrucomicrobiales (V,V)
Bacteroidales (B,B)
Erysipelotrichales (F,E)
Turicibacterales (F,B)
Lactobacillales (F,B)
Clostridiales (F,C)
Family
Prevotellaceae (B,B,B)
Bacteroidaceae (B,B,B)
S24-7 (B,B,B)
Erysipelotrichaceae (F,E,E)
Turicibacteraceae (F,B,T)
Lactobacillaceae (F,B,L)
Peptostreptococcaceae (F,C,C)
Peptococcaceae (F,C,C)
Clostridiaceae (F,C,C)
Lachnospiraceae (F,C,C)
Ruminococcaceae (F,C,C)
Unclassified (F,C,*Clostridiales*)
Verrucomicrobiaceae (V,V,V)
Desulfovibrionaceae (P,Δ,D)
Unclassified (T,M, *RF39*)
Bifidobacteriaceae (A,A,B)
Genus
Desulfovibrio (P,Δ,D,D)
Unclassified (T,M,RF,*unc*)
Akkermansia (V,V,V,V)
Bacteroides (B,B,B,B)
Prevotella (B,B,B,P)
Unclassified (B,B,B,S)
Allobaculum (F,E,E,E)
Turicibacter (F,B,T,T)
Lactobacillus (F,B,L,L)
Unclassified (F,C,C,Ps)
Unclassified (F,C,C,L)
Coprococcus (F,C,C,L)
Unclassified (F,C,C,L)
Ruminococcus (F,C,C,R)
Unclassified (F,C,C,R)
Oscillospira (F,C,C,R)
Clostridium (F,C,C,C)
Unclassified (F,C,C,C)
Unclassified (F,C,C,*unc*)

Figure S6

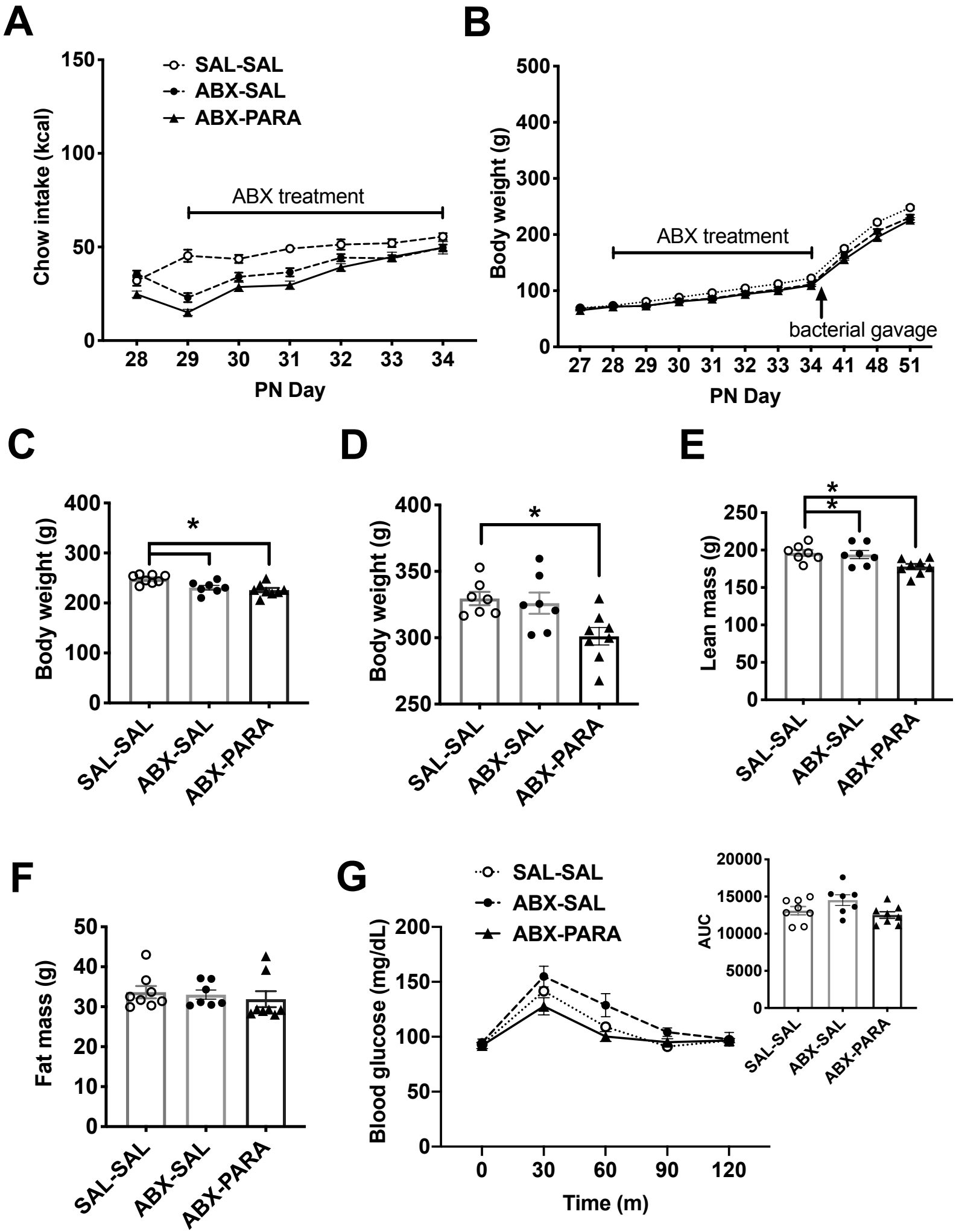
A
SAL-SAL
ABX-SAL
ABX-PARA
Chow intake (kcal)
ABX treatment
PN Day
B
Body weight (g)
ABX treatment
bacterial gavage
PN Day
C
Body weight (g)
SAL-SAL
ABX-SAL
ABX-PARA
D
Body weight (g)
E
Lean mass (g)
F
Fat mass (g)
G
Blood glucose (mg/dL)
Time (m)
AUC

Figure S7

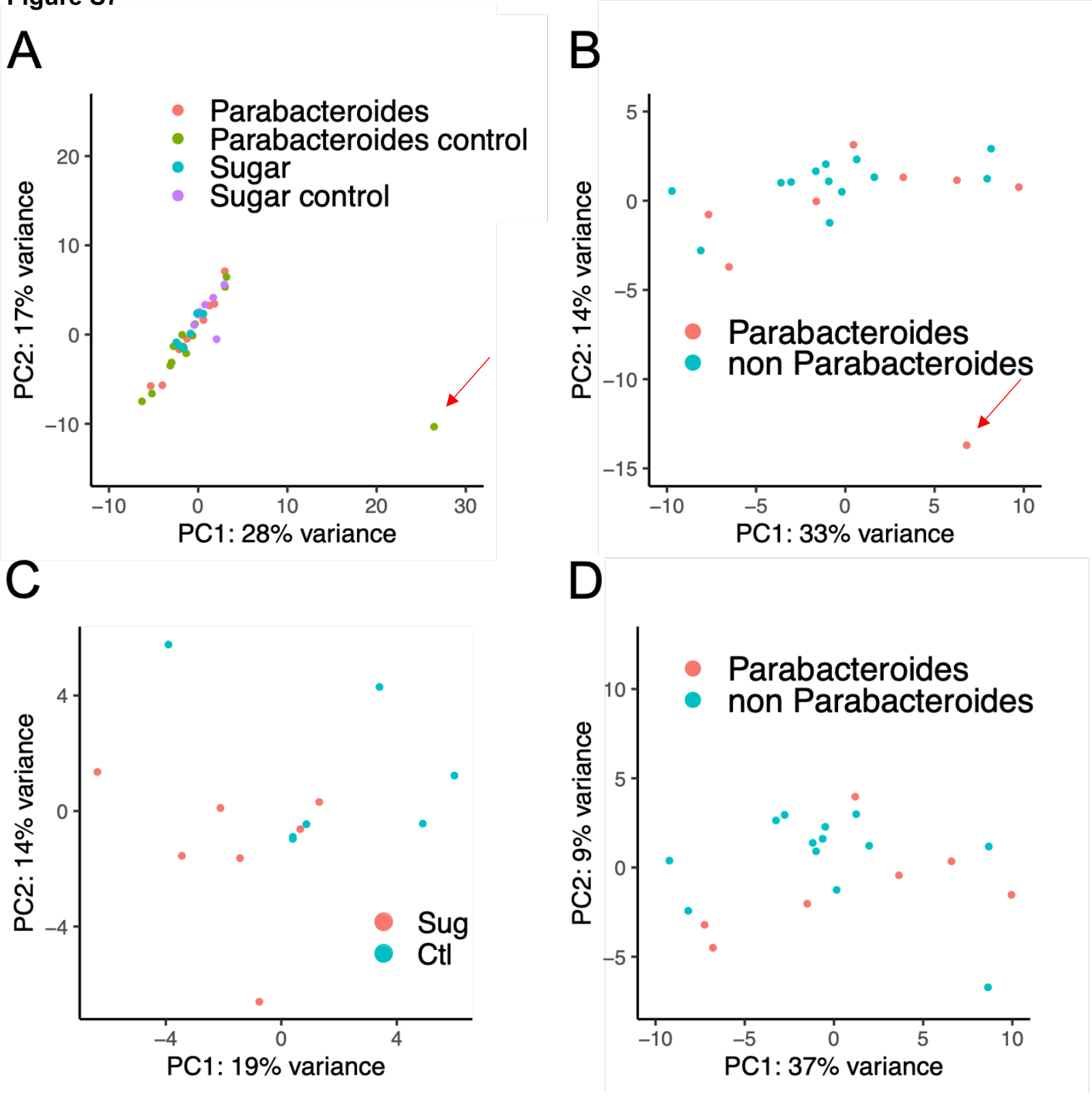
A
Parabacteroides
Parabacteroides control
Sugar
Sugar control
PC2: 17% variance
PC1: 28% variance
B
Parabacteroides
non Parabacteroides
PC2: 14% variance
PC1: 33% variance
C
Sug
Ctl
PC2: 14% variance
PC1: 19% variance
D
Parabacteroides
non Parabacteroides
PC2: 9% variance
PC1: 37% variance

Figure S8

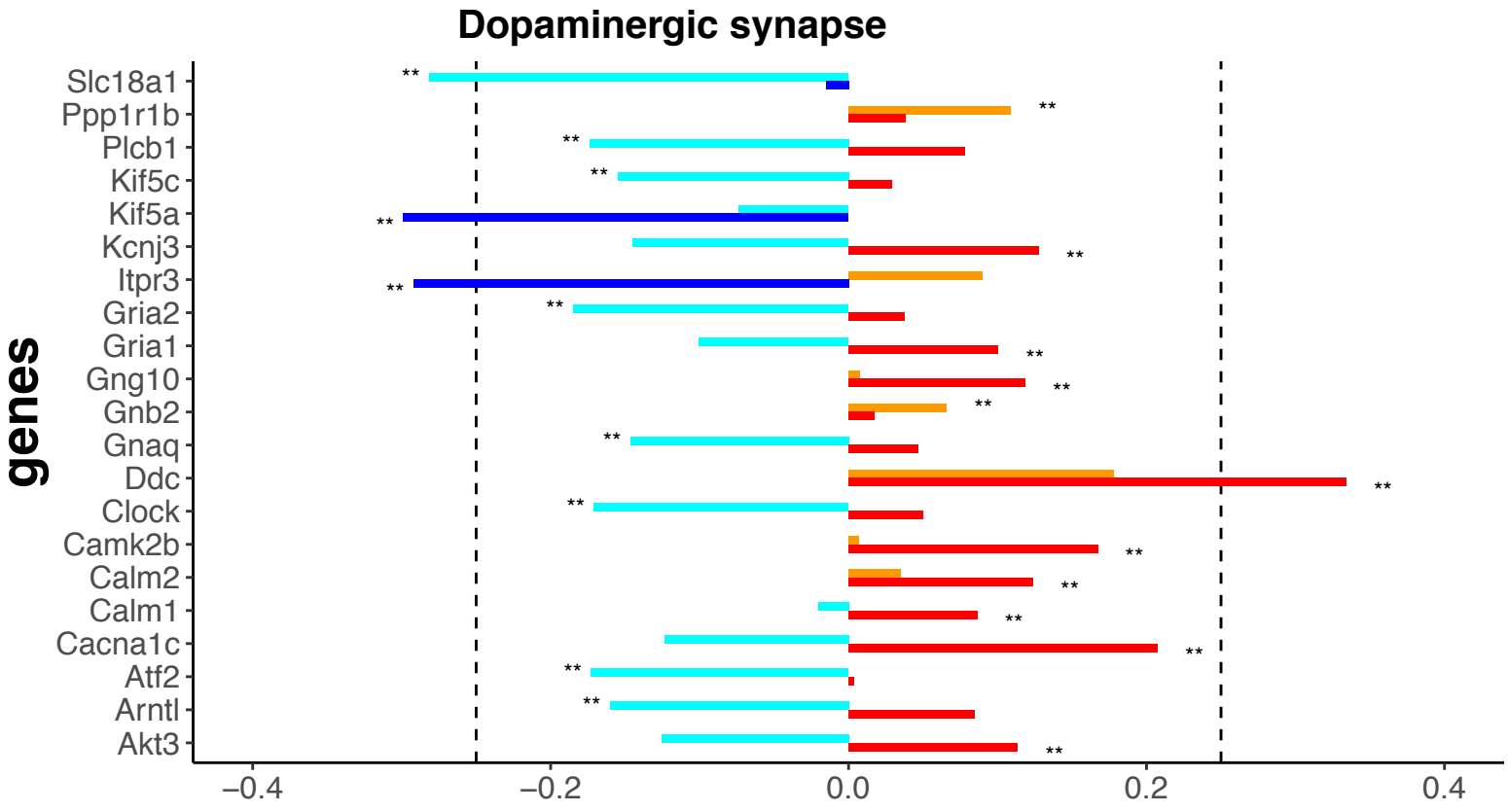
Dopaminergic synapse
genes
Slc18a1
Ppp1r1b
Plcb1
Kif5c
Kif5a
Kcnj3
Itpr3
Gria2
Gria1
Gng10
Gnb2
Gnaq
Ddc
Clock
Camk2b
Calm2
Calm1
Cacna1c
Atf2
Arntl
Akt3
−0.4
−0.2
0.0
0.2
0.4